Construction and Building Materials 369 (2023) 130489

Contents lists available at ScienceDirect

Construction and Building Materials

journal homepage: www.elsevier.com/locate/conbuildmat

Review

A review of concrete properties under the combined effect of fatigue and corrosion from a material perspective

Dongyun Liu [a], Chao Wang [a,*], Jaime Gonzalez-Libreros [a], Tong Guo [b], Jie Cao [a], Yongming Tu [a,b], Lennart Elfgren [a], Gabriel Sas [a,c]

[a] Division of Structural and Fire Engineering, Department of Civil, Environmental and Natural Resources Engineering, Luleå University of Technology, 97187 Luleå, Sweden
[b] Key Laboratory of Concrete and Prestressed Concrete Structures of Ministry of Education, National Engineering Research Center for Prestressing Technology, School of Civil Engineering, Southeast University, 211189 Nanjing, P.R. China
[c] SINTEF Narvik AS, Narvik 8517, Norway

ARTICLE INFO

Keywords:
Concrete
Fatigue load
Corrosion
Combined action
Carbonation
Chloride attack
Freeze–thaw cycles
Sulphate attack
Deterioration
Modelling

ABSTRACT

When in use, reinforced concrete bridge structures not only experience high-frequency fatigue loading caused by passing vehicles, but also suffer from the effects of a corrosive environment. In addition to fatigue damage to reinforcement, long-term fatigue loading also causes concrete cracking and deterioration of pore structures, thereby accelerating the ingress of external corrosive substances and reducing concrete durability. Long-term exposure to a corrosive environment also reduces the performance of concrete and causes corrosion of reinforcement materials, affecting the fatigue performance of the structure. Therefore, there is a combined effect between fatigue loads and corrosion on concrete. This paper is a review of the current literature from a material perspective on the performance degradation of concrete under the combined action of fatigue loading and corrosion, that is, carbonation, chloride ion attack, freeze–thaw cycles, and sulphate attack. The paper includes (1) a description of a test method for examining the combined action of fatigue loading and corrosion, (2) a summary of performance degradation of concrete under the combined effect of fatigue loading and corrosion, and (3) an introduction to durability deterioration models considering fatigue damage, and fatigue models that can account for corrosion. Finally, potential future research on concrete under the combined effect of fatigue loading and corrosion is described.

1. Introduction

As the world's most widely used and important building material, concrete has many advantages, including high compressive strength, easily available and easy to shape [1]. Reinforced concrete structures can be formed by combining concrete with reinforcement materials, as both have similar thermal expansion coefficients [2]. Such techniques have been extensively used in houses, bridges, dams, and for some infrastructure. However, during long-term use, reinforced concrete structures often suffer corrosion from various harsh environments, and have several durability issues, including carbonation, chloride attack, freeze–thaw cycle (FTC) damage and sulphate corrosion. Both carbonation and chloride attack have little effect on the properties of the concrete itself, and the strength and compactness of carbonated concrete can even increase due to the generation of carbonate salt [3]. However, the internal alkalinity of concrete due to carbonate ingress decreases, causing the destruction of the passive film on reinforcement surfaces [4,5]. Then, under the combined action of external moisture, oxygen or chloride ions, corrosion of the reinforcement materials occurs, which seriously threatens the service life of the structure [6]. Unlike carbonation and chloride attack, FTCs and sulphate corrosion mainly damage the concrete itself, resulting in cracking and microstructure loosening, along with a reduction in strength and stiffness of the structure [7,8].

Importantly, reinforced concrete is usually subjected to the combined actions of two or more corrosion factors rather than only a single action. These factors tend to amplify each other, causing even more serious damage to the reinforced concrete. For example, carbonation can increase the concentration of free chloride ions inside the concrete since carbon dioxide can react with Friedel's salt to convert bound chlorides to free chlorides [9,10]. The microcracks caused by FTCs or sulphate

* Corresponding author.
E-mail address: chao.wang@ltu.se (C. Wang).

https://doi.org/10.1016/j.conbuildmat.2023.130489
Received 19 October 2022; Received in revised form 18 January 2023; Accepted 19 January 2023
Available online 31 January 2023

attack can exacerbate the ingress of external carbon dioxide or chloride ions [11,12]. Addit,ionally, along with corrosion, over its lifetime, the reinforced concrete structure will also be subjected to various loads. Durability issues caused by corrosion can lead to a reduction in the strength of concrete and corrosion of reinforcement materials, all of which can adversely affect the load-bearing capacity of the structure. Damage to the structure under long-term loading, mainly cracks, also exacerbates the ingress of external corrosive substances, resulting in more serious durability problems [13]. Therefore, there is a combined effect for concrete structures subjected to loading and corrosion, with these two actions exacerbating each other to cause the failure of the structure.

There have already been some studies into the combined action of static loading and corrosion. Sustained loading action, from a microscopic perspective, changes the distribution of pore size and porosity inside the concrete. Under compressive stress with a low stress level, the change in pore structure is small, and some microcracks can even close due to the compression, thus hindering the transmission of external corrosive substances [14]. However, microcracks occur when the stress level reaches a threshold value, causing an increase in the transport rate of external corrosive substances [15]. For tensile stress, once the level of tensile stress acting on the concrete is greater than the tensile strength of concrete, cracking occurs, accelerating the transport of external corrosive substances. The transport rate increases as the tensile stress level increases [16]. Under the action of bending loads, the compression and tension zones in concrete members exhibit different transport behaviours, and the transport rate of carbon dioxide or chloride ions in the latter is significantly greater than in the former [17]. With an increase in bending load level, the transport rate of substances in the tension zone increases nonlinearly while decreasing in the compression zone [18].

Some reinforced concrete structures, such as highway and railway bridges, are mainly subjected to high-frequency fatigue loadings induced by vehicles or trains instead of static loading. The stress level of fatigue loading is generally low compared to that of static loading. However, repeated fatigue loading leads to the fatigue growth of microcracks and pores inside the concrete, intensifying the ingress of external corrosive substances [19,20]. In addition, due to the complexity of designing a loading test device to measure the coupled actions of corrosion and fatigue load, at present, there are relatively few studies on this compared with studies on the coupling effect of static loading and corrosion. Most studies use one-time or multiple alternating test methods and other indirect methods to study the combined effect of fatigue loading and corrosion. Therefore, in this review, in addition to the introduction of the research background about this topic in this section, the development in fatigue studies and models of concrete is briefly described in Section 2. Then, test methods for the combined effect of fatigue loading and corrosion are described in Section 3. After this, experimental results, and simulation studies of the combined effect of fatigue loading and corrosion from extant literature are summarized in Sections 4 to 7, including the combined effect of fatigue loading and carbonation, chloride ion attack, FTCs, and sulphate corrosion. Finally, the potential for experimental and simulation studies on this topic are discussed, and important conclusions drawn.

2. Brief introduction to concrete fatigue

2.1. Fatigue research and model

Fatigue is the deterioration of a material subjected to repeated loading and unloading, that is, cyclic loading, resulting in progressive and localized damage [21]. Studies of fatigue properties in engineering materials began in the 19th century, but mainly focused on the fatigue of metal materials, such as mine hoist chains, and railway axles. [22,23]. At the beginning of the 20th century, fatigue studies into concrete materials began, including compressive fatigue and flexural fatigue [24–26]. The Wöhler curve [23], or *S*—*N* curve, was the first fatigue model, and was used for metallic materials in the crack initiation phase. It reflects the relationship between the maximum stress level and the number of ultimate fatigue cycles. As with metal materials, the *S*—*N* curve of concrete can be obtained by fitting experimental data. In 1973, an *S*—*N* curve for concrete under compressive fatigue load was proposed by Aas-Jakobsen [27], and then was modified by Tepfers et al. [28], as shown in Eq. (1). This equation is considered to be definitive and widely used and applied in design codes such as fib B52 (2010) [29] and EC2 (2004–2006) [30]. Subsequently, based on this model, some *S*—*N* models for concrete that accounted for various factors such as the minimum stress level [31], concrete strength [32] and loading rate [33] have also been established, including fatigue life models that account for environment corrosion (described in subsequent Sections in this review).

$$S_{\max} = \frac{\sigma_{\max}}{f_c} = 1 - \beta(1 - R)\log N \tag{1}$$

where $S_{\max}$ is the maximum applied stress level, that is, the ratio of maximum concrete stress $\sigma_{\max}$ and the concrete strength f_c, R is the ratio between the minimum stress $\sigma_{\min}$ and maximum stress $\sigma_{\max}$, N is the number of fatigue cycles to failure, and β is a constant which depends on the materials and is approximately 0.0685.

Due to the complexity of test implementation, it is difficult to carry out tensile fatigue tests of concrete [34]. Initial studies of concrete tensile fatigue are often replaced by measuring splitting strength [35]. In 1984, Cornelissen et al. [36] performed the uniaxial repeated tension tests of plain concretes by means of a direct tensile method to obtain the tension fatigue life of the concrete and found that the dispersion of concrete tensile strength would lead to the dispersion of fatigue life results, and established a fatigue S—N curve accounting for tensile strength, as shown in Eq. (2).

$$\log N = 14.81 - 14.52\frac{f_{t,\max}}{f_t} + 2.79\frac{f_{t,\min}}{f_t} \tag{2}$$

where $f_{t,\max}$, $f_{t,\min}$, and f_t are maximum tensile stress, minimum tensile stress, and tensile strength of concrete, respectively.

2.2. Fatigue damage of concrete

The response of concrete under fatigue loading types such as residual strain or residual deformation, has three phases. There is an increase in the number of loading cycles, the rapid development stage, which accounts for about 10 % of the whole response. There is a slow development phase, which accounts for about 80 % of the whole response, and then accelerated development to failure, accounting for only 10 %, as shown in Fig. 1 [37]. Based on the evolution law of fatigue deformation, a deformation-based criterion of fatigue failure was proposed by Balázs [38] and tested by Thun [39], who found that the deformation at peak load during a static test, i.e. $\delta(f_{peak})$ in Fig. 1, corresponds the deformation, $\delta_{2\text{-}3}$, where the failure process begins in a fatigue test i.e. at the changeover point between phases two and three.

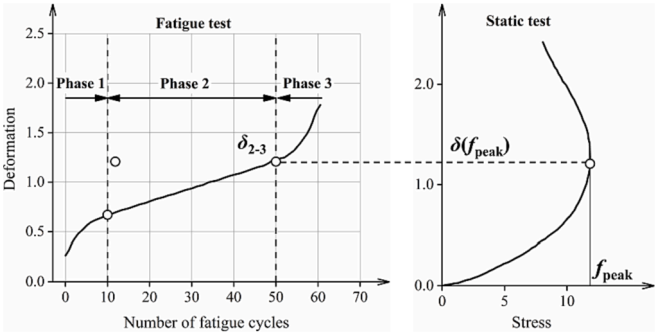

Fig. 1. Deformation fatigue process under repeated loading [37].

In addition, the cumulative fatigue damage theory, the Palmgren-Miner failure hypothesis [40], was developed and applied to gauge fatigue failure of concrete. The hypothesis assumes that the fatigue damage is linearly accumulated with an increase in the number of fatigue cycles. Therefore, the fatigue damage can be defined as shown in Eq. (3).

$$D = \sum \frac{n_i}{N_i} \tag{3}$$

where, D is the degree of fatigue damage, i is a specific stress level, n_i is the number of loading cycles at a specific stress level i, and N_i is the number of load cycles that results in failure at stress level i. When total damage $D = 1$, it is considered that fatigue failure of concrete has occurred. To account for the effect of loading history on fatigue damage accumulation, some modified and nonlinear Palmgren-Miner models have also been developed [41,42]. Since this review mainly focuses on studies of the performance degradation of concrete under the combined effects of fatigue loading and corrosion, there is only a brief introduction to concrete fatigue. Further reviews of fatigue studies into concrete materials/structures can be found in other literature [21,34,43].

3. Test methods to measure combined effect of fatigue loading and corrosion

In real-world conditions, the development of fatigue and durability damage in concrete structures is very slow. Laboratory loading and rapid durability tests are often used to simulate natural usage conditions in order to study the behaviour of concrete under mechanical loading in a corrosive environment. Common laboratory concrete durability tests include rapid carbonation tests, accelerated salt immersion tests, drying-wetting cycle tests and rapid FTC tests. Studies into the performance deterioration of concrete under the combined action of mechanical loading and a corrosive environment suffer from the lack of existing standard test methods, so the following three test methods are generally used. The first is the one-time alternating simulation test, so carrying out durability tests following loading or loading tests after environmental exposure. The second is the multiple alternated simulation test, where the mechanical loading and durability tests are alternately carried out many times. The third method involves the simultaneous test of mechanical loading and environmental exposure. A test method to determine the effect of compressive and tensile stress on chloride ion diffusion was recommended by RILEM TC 246-TDC [44], and the schematic diagram of the test setup is shown in Fig. 2. The test design can simulate the transport of chloride ions in concrete under constant compressive or tensile stress. After the concrete specimen is mechanically loaded with the designed tensile or compressive load, the container containing the chloride salt solution is then fixed to the surface of specimen so that the concrete is subjected to the ingress of chloride ions. Specific test instructions and details can be found in the literature [44].

Since it is easy to apply a constant load, there are many devices for testing concrete under the coupling action of static loading in a corrosive environment [13,45,46], as shown in Fig. 3, Fig. 4 and Fig. 5. Compared with static loading, the actual operation and application of fatigue loading to concrete are more complicated. At present, research into concrete under the combined action of fatigue loading in a corrosive environment mostly uses the one-time alternating simulation test, as shown in Table 1, Table 3, Table 5, and Table 7 in the subsequent Sections in this review. The one-time alternating simulation test is simple to operate, and the loading stress level is easy to control. It is assumed for this test method that the concrete is not subject to environmental corrosion until a certain degree of fatigue damage occurs or does not suffer from fatigue loading until exposed to a corrosive environment for a certain period. Obviously, it does not reflect the real-world conditions of concrete structures. From the beginning of usage, fatigue loading and

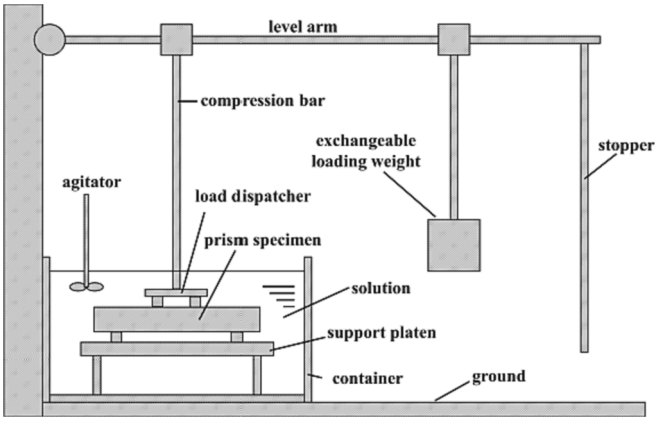

Fig. 3. Combined test of flexural loading and chemical reactions from [45].

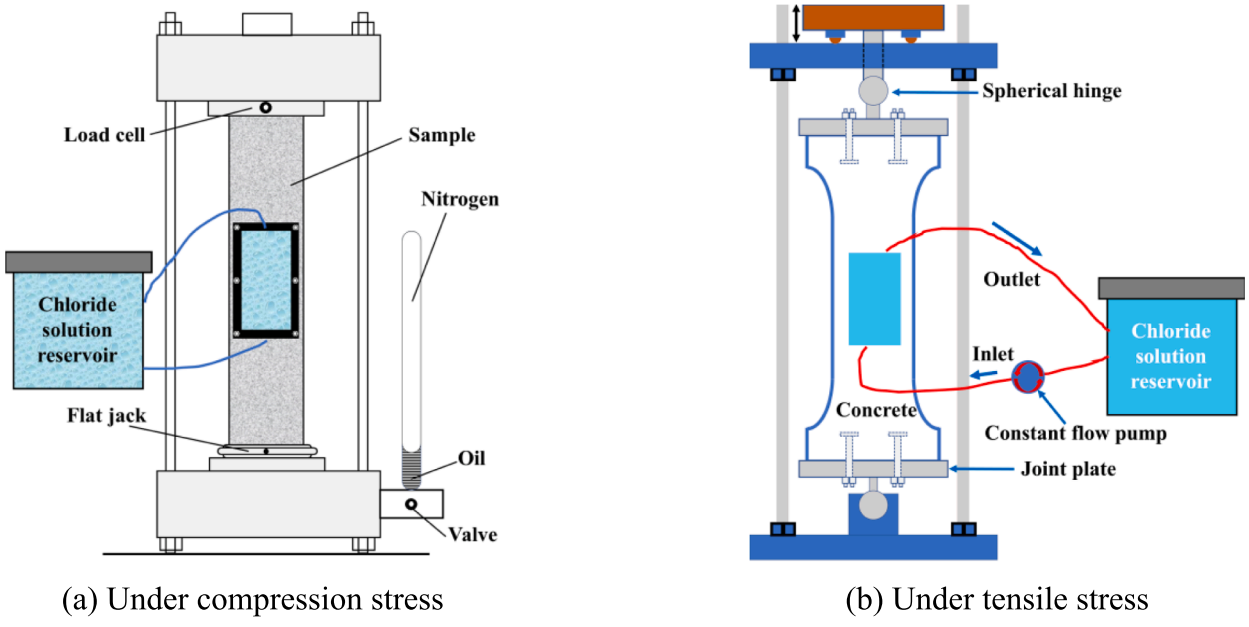

Fig. 2. Test equipment of chloride diffusion test under compression and tensile stresses from [44].

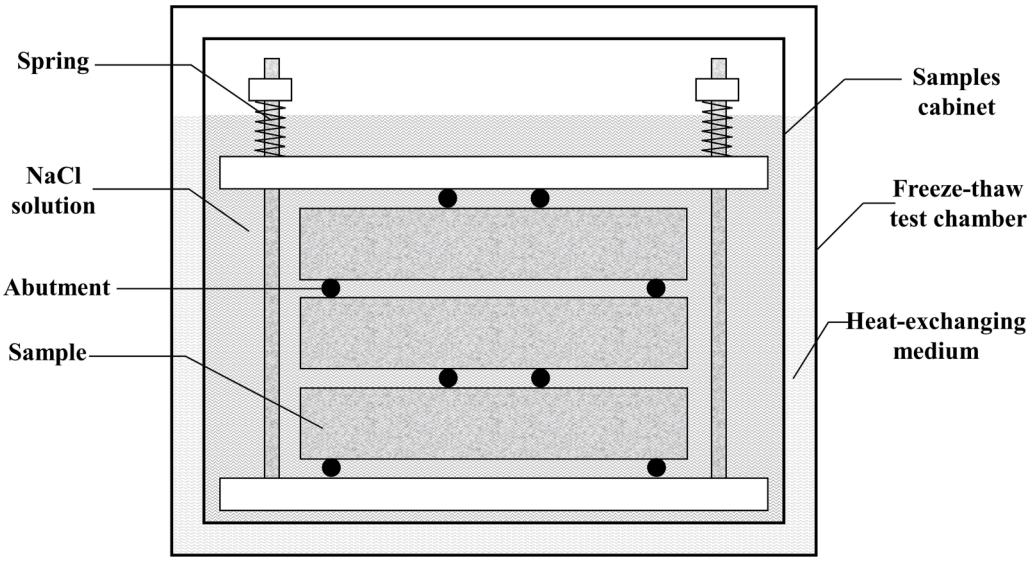

Fig. 4. Combined test of flexural loading and salt FTCs from [13].

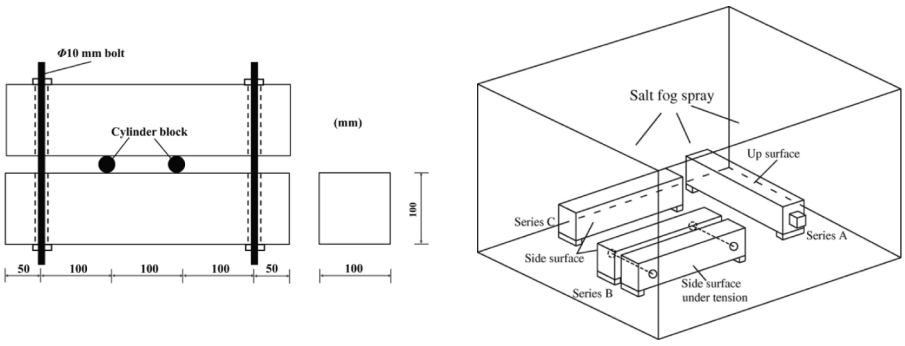

(a) Loading with internal bar tendon (b) Simulation test of salt fog and loading

Fig. 5. Test design of combined action of loading and salt corrosion from [46].

corrosion exposure to the concrete are continuous, and it is by no means the case that the concrete is subjected to one action after suffering from another. Therefore, the test results obtained by using this test method may overestimate the resistance to fatigue and corrosion of concrete.

However, at present, studies into achieving real simultaneous testing of fatigue loading and corrosion are very limited. Compared with chloride or sulphate attack, the simultaneous test of carbonation and fatigue loading is more difficult to carry out, because the corrosive medium of carbonation is carbon dioxide gas and a carbonated environment must be closed. Furthermore, for a carbonation test, it is very important to maintain the specified temperature and humidity. Therefore, it is very difficult to place the fatigue testing machine in the carbonation environment and maintain a constant carbon dioxide concentration, temperature, and humidity. For chloride and sulphate attacks, because the corrosion medium is salt solution, a simultaneous test can be achieved by fatigue loading of concrete specimens in the salt solution container [47,48], as shown in Fig. 6 and Fig. 7. At present, only Li et al. [49] and Qiao et al. [50] have achieved a simultaneous test of FTCs and fatigue loading, by combining a fatigue testing machine with a temperature chamber, as shown in Fig. 8. However, the freeze–thaw environment is closed air FTCs into which no moisture should be allowed to enter, which is somewhat different from water or salt FTCs

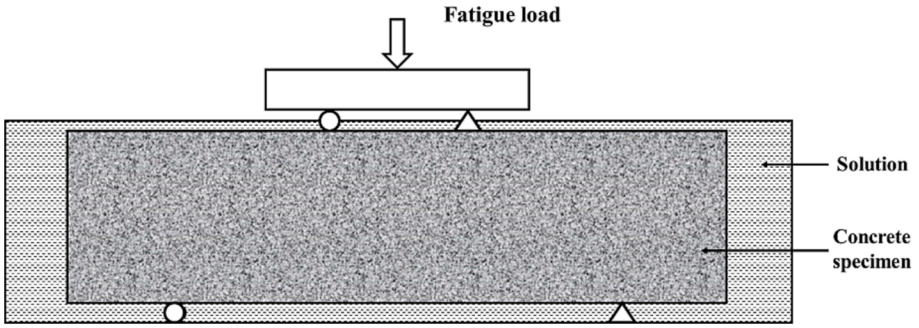

Fig. 6. Design for simultaneous testing of fatigue loading and chloride attack [47].

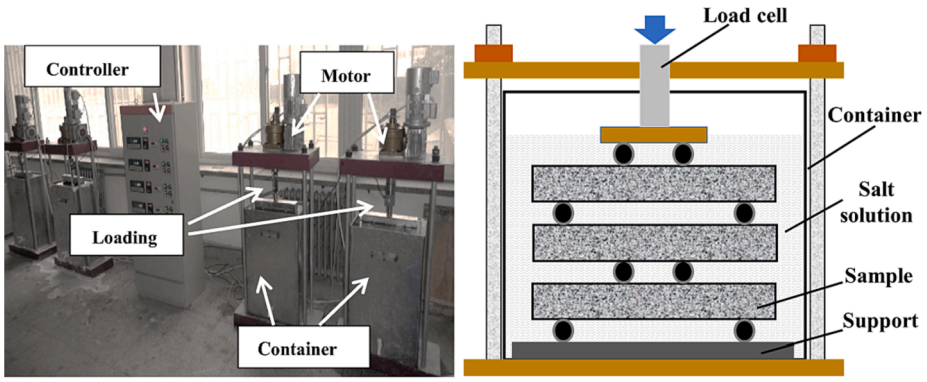

Fig. 7. Design for simultaneous testing of fatigue loading and sulphate attack [48].

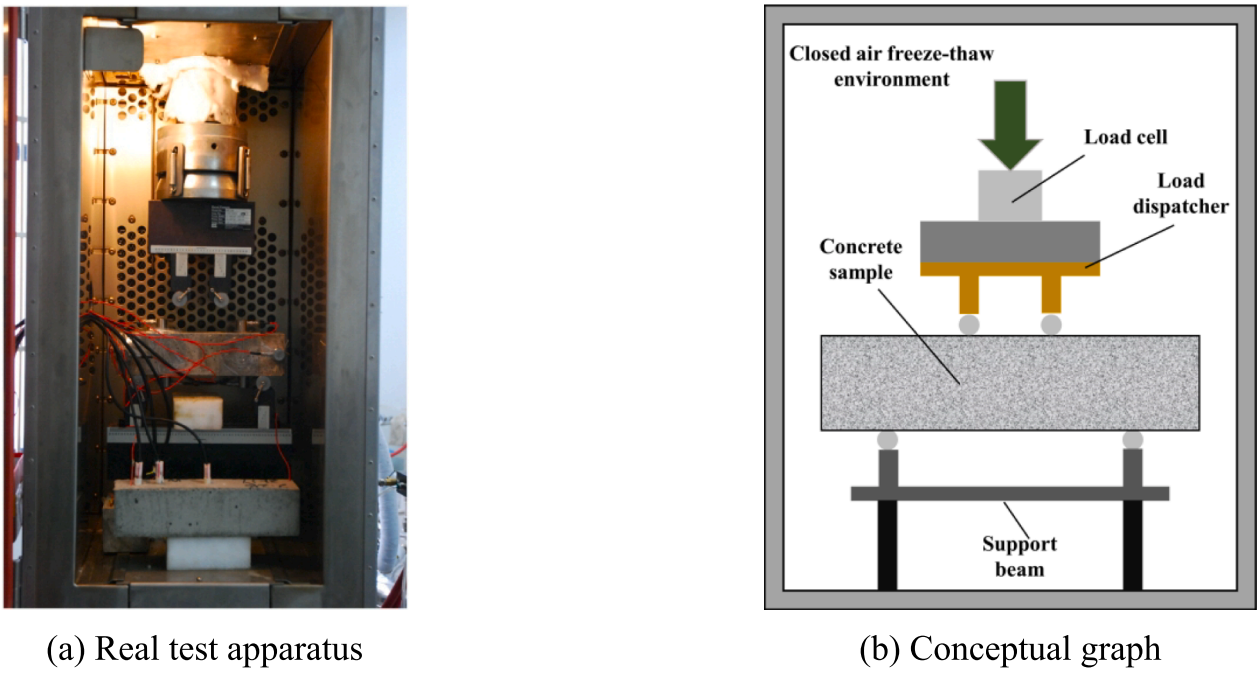

Fig. 8. Simultaneous testing of fatigue loading and freeze–thaw cycles in a temperature chamber [49].

that occur in real life. It is considered that, in addition, the corrosion process is slow, and the fatigue loading is intermittent, so a multiple alternated simulation test has been suggested by some studies [51–53], including in the alternating testing of fatigue loading and freeze–thaw cycles or sulphate attack, one of which is as shown in Fig. 9. However, there are limited studies used multiple alternated simulation tests of fatigue loading in corrosive environments at present. Compared with the simultaneous test, this test method is more flexible, suitable for different corrosive environments, and even the coupling of multiple environmental factors and fatigue loading.

4. Combined effect of fatigue loading and carbonation

4.1. Concrete carbonation

Carbonation is one of the main factors that cause a deterioration in the performance of reinforced concrete structures and happens more often than chloride attack and FTCs [54]. Carbon dioxide in the atmospheric can diffuse into the concrete through connected pores and defects, such as microcracks caused by autogenous shrinkage or drying shrinkage, and dissolve in the pore solution to form carbonate and bicarbonate ions [55]. Subsequently, these substances can react with main hydration products, such as calcium hydroxide, C—S—H gels, and even unhydrated tricalcium silicate and dicalcium silicate, to form calcium carbonate and other salts, thus resulting in a decrease in alkalinity of the concrete [56]. Therefore, concrete carbonation is also referred to as the neutralization reaction of concrete. Generally, the carbonation process has little effect on the properties of the concrete material itself, and even improves the internal pore structures and increases the density due to the generation of carbonation salts [3]. However, when the carbonation is close to the surface of reinforcement material embedded in the concrete, the pore solution with a low pH value can make the passivation film on its surface unstable, eventually destroying it and causing corrosion of the reinforcement material. Different from chloride-induced steel corrosion, the concrete carbonation leads to the uniform corrosion of reinforcement surface [57]. The corrosion mechanism caused by carbonation is shown in Fig. 10. In addition, expansion in the corrosion products will cause cracking of the concrete matrix [58], further accelerating the ingress of external corrosive substances and threatening the overall bearing capacity of the concrete structure.

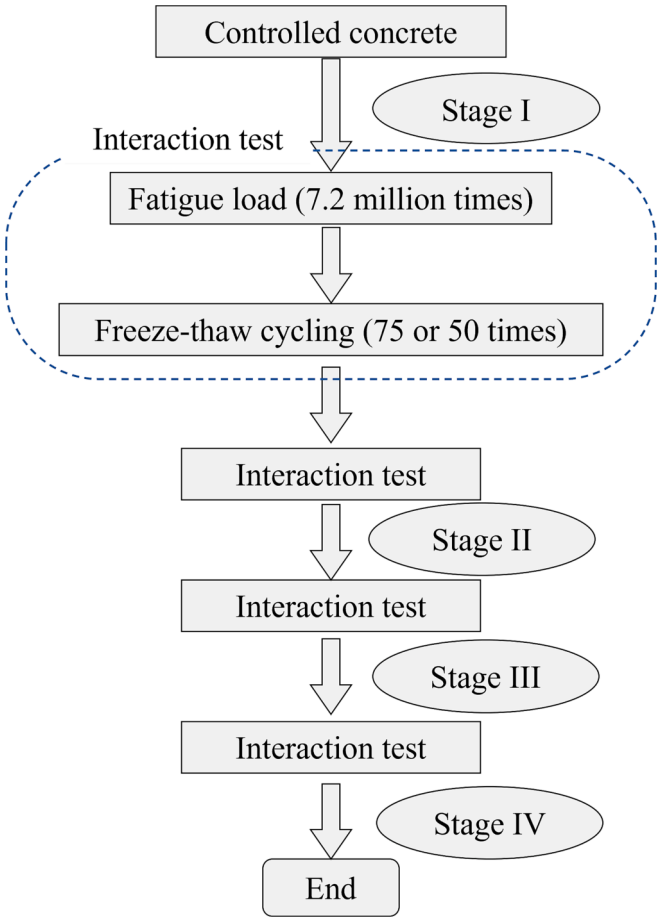

Fig. 9. Alternating testing of fatigue loading and freeze–thaw cycles [51].

There are many factors that affect concrete carbonation, including the cement type, curing condition, concentration of carbon dioxide, environment temperature and relative humidity. The better resistance to penetration, the greater the compactness, and the lower the diffusion rate of carbon dioxide and degree of carbonation. As the ambient temperature increases, the carbonation rate increases [59]. It first increases and then decreases with increases in ambient relative humidity. This is because when the relative humidity is low, the interior of the concrete is very dry, meaning that carbon dioxide has difficultly in dissolving thus hindering carbonation. When the relative humidity is high, the saturated moisture inside the concrete may inhibit the diffusion of carbon dioxide. Studies have shown that when the relative humidity is 60–65 %, the degree of carbonation in concrete can reach the maximum value [3]. The concentration of carbon dioxide is the main factor driving the diffusion of carbon dioxide into concrete. A higher concentration of carbon dioxide results in both a higher rate and a higher degree of carbonation. With the increase in global concentrations of carbon dioxide in the atmosphere, the carbonation of concrete cannot be ignored [60]. Furthermore, cracks in concrete caused by autogenous shrinkage, drying shrinkage, external loading and other factors also accelerate concrete carbonation. However, when the crack width is less than 9 μm, the cracks have little effect on concrete carbonation [61]. The stress state of concrete is also an important influencing factor affecting concrete carbonation. Compressive stress at low stress levels has a positive effect on carbonation resistance, but tensile stress can increase the degree of concrete carbonation [17].

4.2. *Effect of fatigue loads on concrete carbonation*

Concrete structures used in offshore and marine environments, such as bridges, not only carry the dead load from their own weight, but also mostly bear the low/high-frequency fatigue loading created by vehicles or trains. Therefore, it is necessary to study the combined effect of fatigue loading and carbonation, especially when trying to understand the effect of fatigue loading on concrete carbonation. However, because there is the obvious difference between the fatigue loading frequency and carbonation time, that is, fatigue is a high-frequency action while concrete carbonation is a slow process, it is difficult to devise a simultaneous coupling test for these two effects. Therefore, existing studies into the effect of fatigue loading on concrete carbonation all use an experimental design where the carbonation test is carried out after applying a fatigue load for a certain number of cycles to the concrete, as indicated in Table 1. Jiang [70] pointed out that, however, this alternating test design, where the concrete specimen is first subjected to fatigue loading and then carbonation corrosion, ignores the influence of the elastic deformation of the concrete on the diffusion of carbon dioxide. After completing the fatigue loading, elastic deformation of the concrete can recover and the corresponding elastic cracks may be closed, which can reduce the degree of carbonation of the concrete. Based on this, a test design where the static loading and carbonation are carried out simultaneously after fatigue loading has been proposed in order to retain the cracks caused by fatigue loading [70]. Song et al. [69] also

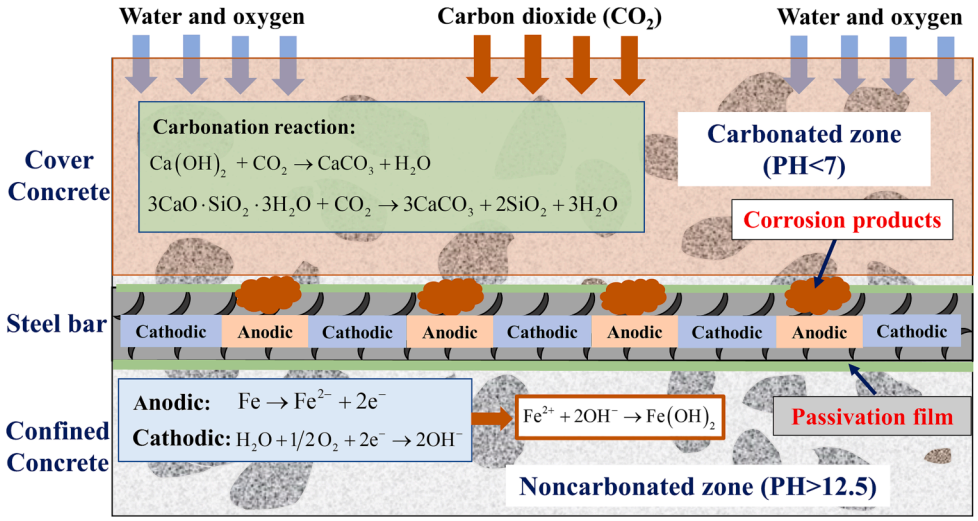

Fig. 10. Corrosion mechanism caused by concrete carbonation.

Table 1
Experimental studies into the effect of fatigue loading on carbonation of concrete from the literature.

Literature	Year	Specimen size (mm)	Combined test methods*	Fatigue loading type	Max. stress level	Loading frequency (Hz)	Fatigue damage index
Tanaka et al. [62]	1999	100 × 100 × 400	F + C	Four-point flexural	0.3, 0.4, 0.5, 0.6, 0.7	5	Dynamic modulus Pore structures
Jiang et al. [63]	2006	100 × 100 × 300 100 × 100 × 400	F + C F + S + C	Uniaxial compressive flexural	0.65	10	Number of fatigue cycles
Wang [64]	2008	100 × 100 × 400	F + C	Four-point flexural	0.65	10	Residual strain
Jiang et al. [65]	2015	150 × 150 × 600	F + C	Four-point flexural	0.8	10	Residual strain
Zhou et al. [66]	2016	150 × 150 × 550	F + C	Four-point flexural	0.5	4	Residual strain
Jiang et al. [67]	2017	100 × 100 × 300	F + C	Uniaxial compressive Eccentric compressive	0.6, 0.7, 0.8	10	Residual strain
Han et al. [68]	2017	100 × 100 × 400	F + C	Four-point flexural	0.55, 0.6, 0.7, 0.8	80	Number of fatigue cycles
Miao et al. [71]	2019	150 × 150 × 550	F + C	Four-point flexural	0.65, 0.7, 0.75	4	Residual strain
Song et al. [69]	2020	150 × 200 × 1500	F + S + C	Four-point flexural	0.4	4	Number of fatigue cycles Pore structures

* In this table, "F + C" denotes that concrete specimens were first subjected to fatigue loading and then carbonation erosion; "F + S + C" denotes that concrete specimens were first subjected to fatigue loading and then the combined action of static loading and carbonation.

used this updated test method to show that the bridge structure was not subjected to fatigue loading all the time, and the duration of fatigue loading was much shorter than that of carbonation. Therefore, the effect of carbonation on fatigue loading can be ignored. However, static loading and carbonation always coexist. So, in laboratory simulations, static loading and carbonation need to be carried out simultaneously.

It can be expected that the resistance to carbonation of the concrete decreases after being subjected to fatigue damage, and the depth and rate of carbonation increase with the increase in degree of fatigue damage. Residual strain [64–67], dynamic elastic modulus [62], number of fatigue cycles [63,68 69], and pore microstructure [62,69] are the main indicators that characterize fatigue damage of concrete in the extant literature, as shown in Table 1. Wang [64] found that, with the increase of degree of fatigue damage, the carbonation depth continued to increase, particularly when the ratio of residual strain to ultimate residual strain exceeded 0.4, at which point the resistance to carbonation decreased significantly. Miao et al. [71] came to a similar conclusion through experimentation. Jiang et al. [67] pointed out that when the residual strain increases from 0 to 0.002, the carbonation rate increases by 75 %. In addition to promoting the formation and propagation of microcracks, fatigue loading also significantly affects the pore structure inside the concrete. With an increase in the number of fatigue cycles, the volume of capillary pores with a diameter less than 50 nm decreases, and the volume of macropores with a diameter greater than 50 nm increases. At this point, the porosity is linearly positively correlated with the degree of fatigue damage which is expressed as the ratio of the number of applied fatigue cycles and ultimate fatigue cycles [69], as shown in Fig. 11. Tanaka et al. [62] found that the dynamic elastic modulus exhibits little change while its pore structure changes significantly after fatigue loading; even with a low-level fatigue stress, the number of pores with the diameters of 10–100 nm and 0.1–5.68 μm increase significantly, which is the main reason for the decrease in resistance to carbonation of the concrete in the stress-damaged zone. Therefore, when studying the effect of fatigue loading on concrete carbonation, in addition to considering the effect of microcracks generated by that loading, it is essential to investigate the change in the internal pore structures after fatigue loading.

The type of fatigue loading also significantly affects the carbonation depth of fatigue-damaged concrete. Fatigue damage caused by axial tensile fatigue and compression fatigue loading in the concrete is relatively uniform [67], therefore, the degrees of carbonation in different parts can be regarded as the same. However, flexural fatigue loading and eccentric compressive fatigue loading [72] can both cause different degrees of damage in different parts [62]. Since the tensile strength of concrete is much lower than its compressive strength, the carbonation depth of concrete in the tension zone is often higher than that in the compression zone [62,67]. When the number of fatigue cycles is low, the

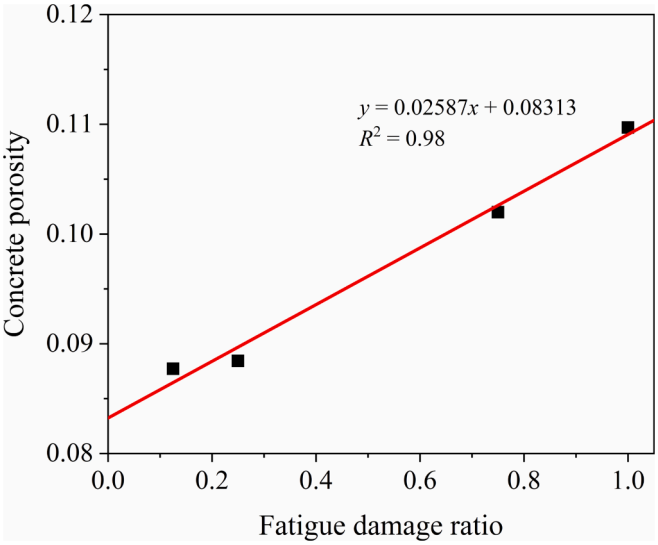

Fig. 11. Porosity of fatigue-damaged concrete [69].

compressive stress may suppress microcracking or micropores in the compression zone and inhibit the carbonation process [14]. However, once the compression fatigue damage reaches a certain level, the carbonation process also increases significantly. Therefore, the non-uniformity of internal damage of concrete specimens caused by eccentric or bending fatigue loading should also be considered in the study of the effect of fatigue loading on concrete carbonation.

4.3. Carbonation model accounting for fatigue load

Fick's first law of diffusion can be used to describe the diffusion of carbon dioxide inside concrete [73,74]. There is a positive proportional relationship between the carbonation depth of concrete and the square root of the carbonation time, as shown in Eq. (4). In addition, existing studies have shown that, for the fatigue-damaged concrete, the carbonation depth also varies linearly with the square root of carbonation duration [67], as shown in Fig. 12.

$$x_c = k\sqrt{t} \tag{4}$$

where x_c is the carbonation depth of concrete, k is carbonation coefficient, and t is carbonation time.

There have been studies into a prediction model for the carbonation depth of concrete in the atmospheric environment, and some empirical models and numerical models examining the influence of various factors

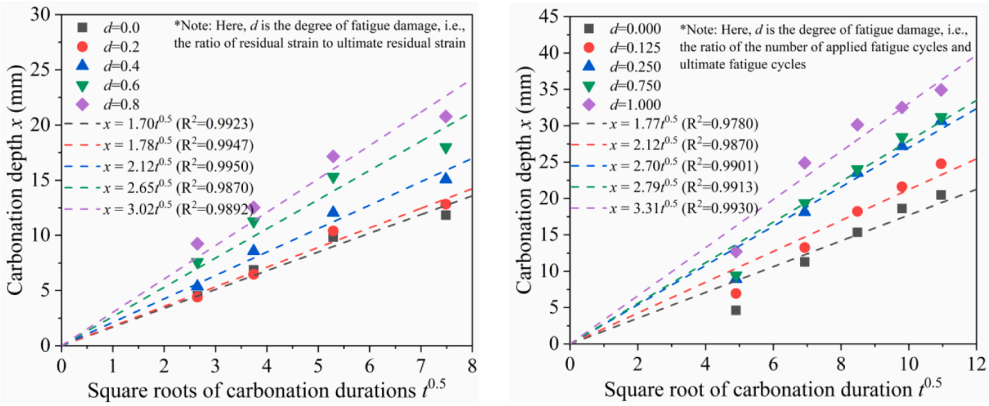

(a) Test data from [71] (b) Test data from [69]

Fig. 12. Carbonation depth of fatigue-damaged concrete with square root of exposure duration.

have been created, including concentration of carbon dioxide [75], temperature and relative humidity of environment [76], cement content [77], and curing conditions [78]. In addition, in recent years, the effect of loading on concrete carbonation has attracted more attention, with some concrete carbonation models that account for different stress states being developed, including axial tensile stress, axial compressive stress, and bending stress [79,80]. Compared with static loading, there are limited studies on the effect of fatigue loading on concrete carbonation and related carbonation models accounting for the fatigue damage.

Table 2 lists the concrete carbonation depth models that account for fatigue damage in the extant literature, including both mathematical and numerical models. Based on the classical carbonation model from literature [81], Jiang et al. [63,70] modified the diffusion coefficient of carbon dioxide by introducing a factor that modelled the influence of fatigue loading and created a concrete carbonation depth model using residual strain as the fatigue damage index. In this model, the total diffusive flux of carbon dioxide in the fatigue-damaged concrete is considered to provide coupling of the diffusive flux of carbon dioxide between the uncracked concrete matrix and the interior of the cracks [82,83]. To simplify the analysis, a conical crack induced by the bending

Table 2
Carbonation models of fatigue-damaged concrete from the literature.

Literature	Year	Model	Annotation	Note
Jiang et al. [63,70]	2006, 2008	$x_c = \sqrt{2C_{CO_2}k_f k_{RH}k_T k_{curing}D_0}\sqrt{t}k_f = 1 + \frac{0.785\varepsilon_r^n D_c}{(\varepsilon_r^n+2)D_0}k_{RH} = 5.45(1-RH)(RH)^{1.5}k_T = \exp\left[\frac{U}{R}\left(\frac{1}{298}-\frac{1}{T}\right)\right]k_{curing} = 5.33t_{curing}^{-0.5}$	x_c = carbonation depth of concrete C_{CO2} = ambient CO_2 concentration k_f = influencing factor of fatigue load k_{RH} = influencing factor of relative humidity k_T = influencing factor of temperature k_{curing} = influencing factor of curing environment D_0 = Benchmark CO_2 diffusivity of undamaged concrete when C_{CO2} = 20 % t = carbonation time ε_r^n = residual strain at n fatigue loading cycles D_c = CO_2 diffusivity in cracks, 8.85×10^{-6} m^2/s theoretically U = activity energy of CO_2 R = ideal gas constant RH = relative humidity T = environment temperature t_{curing} = curing time	• Residual strain as the flexural fatigue damage index Diffusion of CO_2 in fatigue-damaged concrete is treated as a coupling between diffusion in undamaged concrete and diffusion in fatigue cracks Cone-shaped cracks are treated as cylindrical cracks of constant width CO_2 diffusivity in cracks D_c is treated as the average of its diffusion coefficient in air and water
Jiang et al. [65]	2015	Numerical model: $\frac{\partial}{\partial x}\left(D_d\frac{\partial[CO_2]}{\partial x}\right) = \frac{\partial}{\partial t}(\varphi(1-S)[CO_2]) + Q$ $D_d = D_{con} + (1-\lambda)\left(1-\frac{x}{h/2}\right)\cdot\varepsilon_{rm}D_{air}$ $D_{con} = 1.64\times10^{-6}\varphi^{1.8}(1-RH)^{2.2}(0.02T+0.6)$	D_d = CO_2 diffusivity in cracks in fatigue-damaged concrete $[CO_2]$ = molar concentration of CO_2 in the exposed environment φ = porosity of concrete S = pore saturation of concrete Q = total consumption rate of carbonation reaction of concrete D_{con} = CO_2 diffusivity in uncracked concrete λ = proportion of aggregate at concrete h = total depth of sample along the	• Suitable for the tensile zone of beams Residual strain as the fatigue flexural damage index Accounts for the non-uniformity of residual strain along the direction of corrosion Accounts for the effect of coarse aggregates bridging two sides of the crack on the CO_2 diffusivity It is assumed that carbonation occurs after fatigue damage Assuming the reduction factor α is a constant

(continued on next page)

Table 2 (*continued*)

Literature	Year	Model	Annotation	Note
		Simplified model: $x_c = \sqrt{2D_{con}m_0t} + \alpha\sqrt{2(1-\lambda)\varepsilon_{rm}D_{air}m_0t}$	erosion direction ε_{rm} = maximum residual strain at tensile zone D_{air} = CO_2 diffusivity in air m_0 = initial concentration factor α = a reduction factor, 0.25 simplistically	
Miao et al. [71]	2019	$x_c = k_\delta k_f 839(1-RH)^{1.1}\sqrt{\frac{\frac{W}{\gamma_c C}-0.34}{\gamma_{HD}\gamma_c C}}C_{CO_2}\sqrt{t}k_f = 0.519 + 0.455e^{1.255\frac{\varepsilon_r^n}{\varepsilon_r^N}}$	k_δ = adjustment coefficient W/C = Water/cement ratio γ_c = coefficient for cement type γ_{HD} = coefficient of degree of cement hydration C = cement content ε_r^N = ultimate residual strain at N fatigue loading cycles	• Degree of fatigue damage is treated as the ratio of residual strain to ultimate residual strain There is an exponential relationship between the influencing coefficient of fatigue load and degree of fatigue damage
Jiang et al. [72]	2018	Numerical model: $\frac{\partial}{\partial x}\left(D_d\frac{\partial[CO_2]}{\partial x}\right) = \frac{\partial}{\partial t}(\varphi(1-S)[CO_2]) + Q$ $D_d = D_{con} + \lvert\varepsilon_r(x)\rvert(1-\eta\lambda_1(x))D_{air}$ For ordinary Portland cement-based concrete: $D_{con} = 1.64\times10^{-6}\varphi^{1.8}(1-RH)^{2.2}(0.02T+0.6)$ For concrete containing SCMs: $D_{con} = 6.10\times10^{-6}\varphi^{3.0}(1-RH)^{2.2}(0.02T+0.6)$ $D_{air} = 1.03\times10^{-7}T + 1.3557\times10^{-5}$	$\varepsilon_r(x)$ = residual strain at any corrosion depth x $\lambda_1(x)$ = area fractions of aggregates along corrosion depth x η = a reduction factor, 0 for tensile zone, and 0.5 for compressive zone, empirically	• Accounts for the difference in the distribution of residual strain on corrosion depth of different fatigue damage patterns, i.e. uniform compressive, gradient compressive and gradient tensile damage
Song et al. [69]	2020	Numerical model: $\frac{\partial}{\partial x}\left(D_d\frac{\partial[CO_2]}{\partial x}\right) = \frac{\partial}{\partial t}(\varphi(1-S)[CO_2]) + Q$ $D_d = D_{con} + \frac{\omega_m}{l_m}((1-\lambda)D_{air} + \lambda D_{agg})$ $D_{con} = 1.64\times10^{-6}(\varphi(1+0.311d))^{1.8}(1-RH)^{2.2}k_T$	D_{agg} = CO_2 diffusivity in aggregate ω_m = average crack width under fatigue loading l_m = average crack spacing under fatigue loading d = degree of fatigue damage, i.e., the ratio of the number of applied fatigue cycles and ultimate fatigue cycles	• Accounts for the effect of porosity coarsening and cracking caused by fatigue loading on the CO_2 diffusivity

fatigue load in the tensile zone of the concrete specimen is treated as a cylindrical crack with a constant width, and the crack spacing factor is used to describe the crack distribution in the concrete surface. In fact, however, the residual strains and crack widths in the tensile zone of the concrete specimen are not uniformly distributed under bending fatigue loads. Jiang et al. [67] found, through experimental study, that the residual strain of concrete in the tensile zone exhibits a linear decay trend from the surface to the middle of the specimen. Therefore, a numerical model of concrete carbonation depth allowing for the inhomogeneity of residual strain was created [65]. In addition, the way coarse aggregates obstruct the diffusion of carbon dioxide was also considered [72]. Based on this research, a numerical model of concrete carbonation depth accounting for different degrees of fatigue damage was created. Based on the parametric analysis of the results of this model, a simplified carbonation mathematical model that can be directly applied to practical engineering issues where fatigue damage occurs was developed [65]. In addition, Miao et al., [71] found, through experimentation, that there is an exponential relationship between the factor that models the influence of fatigue loading and the degree of fatigue damage characterized by residual strain, and thus developed an empirical model of concrete carbonation depth accounting for the effect of fatigue damage. Song et al. [69] measured the distribution of cracks on the concrete surface and the change of porosity inside the concrete after fatigue loading, and by considering the increase in porosity and the effect of cracking on the diffusion coefficient of carbon dioxide, developed a numerical model of concrete carbonation.

However, the above models all assume that concrete carbonation starts after fatigue damage, which may be inconsistent with real-world conditions. In use, although the carbonation process is slow, it is always occurring. In fact, fatigue loading does not cause obvious damage to the concrete at the initial stage of loading, and only when the damage reaches a certain level can carbonation be significantly accelerated by fatigue loading. Therefore, when considering the coupling effect of fatigue loading and carbonation, the carbonation of concrete can be divided into two stages: the carbonation can be considered as not being affected by fatigue loading in the early stage, but at a later stage, the acceleration effect of fatigue damage on concrete carbonation needs to be accounted for. Therefore, it is important to determine when fatigue damage significantly accelerates concrete carbonation, something which requires further research.

5. Combined effect of fatigue loading and chloride ion attack

5.1. Chloride corrosion of concrete

Chloride ion ingress is one of the main causes of corrosion of the reinforcement materials inside reinforced concrete structures [84]; another is concrete carbonation as mentioned above. Inside the concrete, cement hydration products with high alkalinity can form a dense oxide film on the surface of reinforcement materials, which prevent corrosion of those materials [84]. As chloride ions have a strong depassivation property, when enough chloride ions reach the oxide film through the connected pores and cracks of the concrete, the pH of the surrounding pore solution decreases and the protective film is destroyed, allowing corrosion of reinforcement material to occur [5]. Furthermore, importantly, chloride ions can act as catalysts, driving the corrosion reaction without being consumed themselves [86]. Therefore, chloride ions entering the concrete can continuously damage the concrete structure, which is the main characteristic of chloride corrosion. In addition, different from the uniform corrosion caused by concrete carbonation, the chloride-induced steel corrosion is pitting corrosion [85], and the schematic representation of chloride-induce corrosion is shown in Fig. 13.

The transmission of chloride ions through microcracks and pores inside the concrete is a very complex process, and includes at least six types of action: diffusion, convection, adsorption, electromigration,

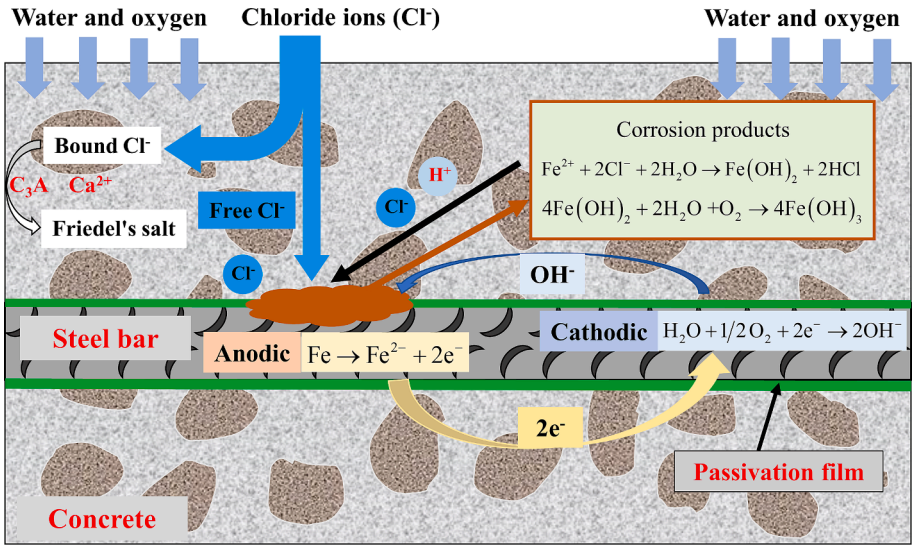

Fig. 13. Schematic representation of chloride-induce corrosion of steel in the concrete.

penetration and capillary [87]. Diffusion, penetration, and capillary action are the common transmission processes, with diffusion being the main process for chloride transport in saturated concrete. Collepardi et al. [88] first established a model for chloride diffusion inside concrete based on Fick's second law of diffusion and based on the assumption that the chloride ion diffusion coefficient is a constant. An analytical solution to this model is shown in Eq. (5).

$$C(x,t) = C_0 + (C_s - C_0)\left(1 - \mathrm{erf}\left(\frac{x}{2\sqrt{Dt}}\right)\right) \quad (5)$$

where $C(x, t)$ is the chloride ion concentration at time t at distance × from the concrete surface, C_0 is the initial chloride ion concentration before exposure, C_s is the chloride ion concentration on the concrete surface, D_a is the chloride ion diffusion coefficient, and erf is an error function. Subsequently, some modified chloride diffusion models based on this model and accounting for the influence of various factors have been proposed. These include factors such as the time dependence of the chloride diffusion coefficient [89], the binding capacity of chloride ions [90], time-varying surface chloride ion concentration [5], the water-cement ratio [91], the aggregate volume fraction of concrete [92], and environmental factors [93]. The chloride diffusion coefficient is an important factor affecting the transmission of chloride ions in concrete. With an increase in the corrosion time, the hydration process of concrete is gradually completed, so the chloride diffusion coefficient gradually decreases [89]. Due to the physical adsorption and chemical binding of cement hydration products to the chloride ions, chloride ions that penetrate the concrete interior can be classified as either free chlorides or bound chlorides, but only the former cause rebar corrosion [94]. Therefore, the effect of the chloride ion binding capacity on the chloride ingress process cannot be ignored.

In addition to the aforementioned influencing factors, concrete structures in offshore and marine environments suffer from the combined effect of loading and chloride attack during their lifetimes. Recently, the effect of loading on chloride ion transmission in concrete has received more attention. Previous studies show that chloride diffusion coefficient first decreases and then increases with an increase in compressive stress [95], and critical compressive stress that can significantly increase chloride diffusion varies from 0.3 to 0.9, depending on the materials, curing, and environment. For a concrete member subjected to flexural loading, as the bending stress level increases, the chloride diffusion coefficient in the tension zone increases, while the chloride diffusion coefficient in the compression zone does not change appreciably [17].

5.2. *Effect of fatigue loading on chloride corrosion*

Similar to the effect it has on carbonation, fatigue loading also accelerates the transmission of chloride ions by deteriorating the pore structure and generating microcracks in the concrete. In addition, it is easy to produce a simultaneous test simulation of static loading and chloride corrosion, while there are fewer studies that describe a simultaneous test of fatigue loading and chloride corrosion. Most experiments carry out a chloride corrosion test after fatigue loading. The relevant studies into the effect of fatigue loading on the chloride corrosion of concrete are shown in Table 3.

Applied loading deteriorates the pore structure inside the concrete and promotes the formation and propagation of microcracks. At the same stress level, fatigue loading can induce more and longer cracks in the concrete than static loading [96], chloride ions can be transported quicker, and internal chloride ion concentration is higher. Saito et al. [97] evaluated the chloride ion permeability of concrete after static and fatigue compressive loading and found that, even when static compressive loads reached 90 % of ultimate load, the chloride permeability of the concrete did not significantly increase. However, when the maximum stress level of fatigue loading reached 60 % of ultimate load, the chloride permeability clearly increased. By studying the durability of reinforced concrete beam under the combined effect of loads and sea water corrosion, and applying constant current to accelerate the corrosion of reinforcement materials, Ahn et al. [96] found that under fatigue loading, corrosion of reinforcement material occurred faster, and the ultimate bearing capacity of beam was lower than that under static loading.

The types of fatigue loading and stress levels significantly affect chloride diffusion in concrete. Under uniaxial fatigue compressive loading, stress levels below 0.5 do not cause a significant increase in the chloride permeability of concrete, but when the stress levels exceed a certain critical value, about 0.6, the chloride diffusion coefficient increases significantly [97]. The results of experiments by Song et al. [98] showed that when the stress level increases to 0.75, the chloride diffusion coefficient of concrete increases very rapidly with the increase of fatigue cycles, as shown in Fig. 14. Similar results were also obtained by Li et al. [99], who pointed out that a critical stress level of 0.7 significantly increases chloride diffusion and found that, when the stress level was 0.5, the chloride diffusion coefficient first decreased and then increased with fatigue cycles as the compressive load closed the internal microcracks at the initial loading stage. From above studies, the critical compressive stress level causing the significant increase of chloride

Table 3
Experimental studies into the effect of fatigue loading on chloride diffusion in concrete from the literature.

Literature	Year	Specimen size (mm × mm × mm)	Combined test methods*	Fatigue loading type	Maximum stress level	Loading frequency (Hz)	Chloride diffusion test method	Fatigue damage index
Saito et al. [97]	1995	100 × 100 × 400	F + CL	Uniaxial compressive	0.5, 0.6, 0.7, 0.8	5	Chloride electric flux test	Residual strain
Wang [64]	2008	100 × 100 × 400	F + CL	Four-point flexural	0.65	10	Chloride salt wet-dry cycles Chloride electric flux test	Residual strain
Wang et al. [109]	2012	70 × 70 × 280 (Mortar)	FCL	Four-point flexural	0.3, 0.4, 0.5	10	Chloride salt immersion	Acoustic emission detection
Ren et al. [47]	2015	150 × 250 × 1800 (RC specimen)	FCL	Four-point flexural	0.34, 0.47, 0.62	1	Chloride salt immersion	Load level
Song et al. [98]	2016	100 × 100 × 400	F + CL	Uniaxial compressive	0.5, 0.6, 0.7, 0.75	5	Rapid chloride migration (RCM) test	Electrical impedance parameter
Niu et al. [105]	2015	150 × 150 × 550	F + CL	Four-point flexural	0.5	4	Chloride salt spray test	Residual strain
Liu et al. [103]	2015	100 × 150 × 700 (RC specimen)	F + CL	Four-point flexural	0.16, 0.24, 0.32, 0.40	4	Chloride salt wet-dry cycles	Crack width
Fu et al. [104]	2016	120 × 120 × 1200 (RC specimen)	F + CL	Uniaxial tension	0.25, 0.3, 0.35, 0.4, 0.45	5	Chloride salt immersion Chloride salt wet-dry cycles	Residual strain
Jiang et al. [111]	2017	100 × 100 × 515	F + CL	Uniaxial tension	0.5, 0.6, 0.7, 0.75	10/5	Modified RCM test	Residual strain Fractal damage index factor Responsive variable resistance
Yu [100]	2017	100 × 100 × 400	FCL	Four-point flexural	0.2, 0.4, 0.6	0.01, 0.02	Chloride salt immersion Chloride salt wet-dry cycles	
Wu et al. [108]	2018	100 × 150 × 800 (RC specimen)	F + CL	Four-point flexural	0.2, 0.3		Chloride salt wet-dry cycles	Load level
Wang et al. [110]	2015	120 × 300 × 1500 (RC specimen)	F + CL	Three-point flexural	0.3 ~ 0.35		Chloride salt wet-dry cycles	Crack pattern
Wu et al. [101,106,107]	2019, 2020, 2021	150 × 250 × 1800 (RC specimen)	F + CL	Four-point flexural	0.2, 0.3, 0.4, 0.5	4.1	Chloride salt wet-dry cycles	Load level Fatigue loading cycles
Jiang et al. [112]	2020	150 × 150 × 300	FCL	Uniaxial compressive	0.75	0.5	Chloride salt immersion	
Li et al. [99]	2022	100 × 100 × 400	F + CL	Uniaxial compressive	0.5, 0.7		RCM test	

* In this table, "F + CL" denotes that concrete specimens were first subjected to fatigue loading and then a chloride ingress test. "FCL" denotes that concrete specimens were subjected to fatigue loading and chloride ingress simultaneously.

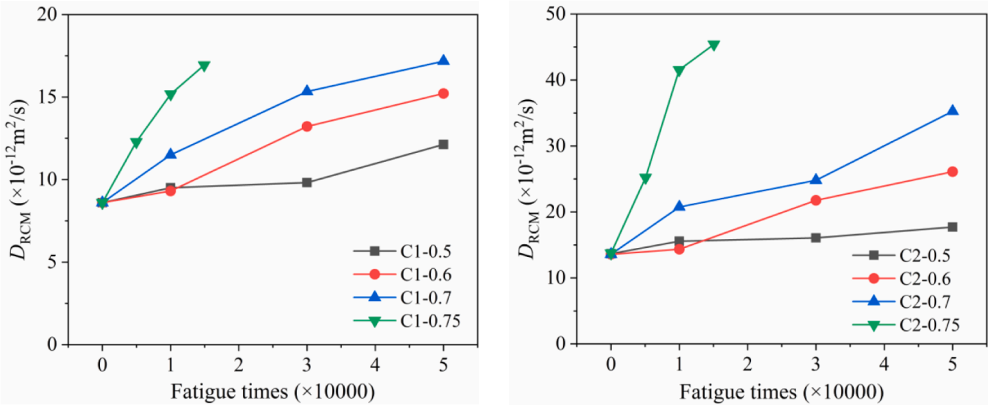

(a) with water-cement ratio of 0.36 (b) with water-cement ratio of 0.50

Fig. 14. Chloride diffusion coefficient with different fatigue stress level (0.5, 0.6, 0.7, and 0.75) in two concretes [98].

diffusion is about 0.6–0.75. Saito et al. [97] obtained that a great number of microcracks will be generated when the compressive fatigue level is more than 0.67, which is the main reason that accelerating chloride ion penetration in the range of such compressive stress level. Studies on the effect of fatigue loads on the diffusion of chloride ions in concrete have mostly focused on bending fatigue load. With the increase of fatigue bending stress level, the diffusion coefficient of chloride ions increases, and the concentration of chloride ions inside the concrete also increases significantly [100]. Wu et al. [101] discussed how the resistance to chloride attack of concrete damaged by high cycle bending fatigue changed, and pointed out that, when the fatigue stress level was greater than 0.3, the chloride ion concentration in the concrete increased significantly. As mentioned in Section 2, the development of cracks and strains in concrete is slow during the second stage of the fatigue damage curve while cracking and damage develop quickly in the first and third stages. Therefore, the initial fatigue loading cycles (first fatigue stage) significantly increase the chloride diffusivity i.e. the chloride concentration increases from 0.002 % to 0.029 % as the fatigue loading increases from 0 to 0.2 million cycles, while the loading cycles (~0.4–1.2 million cycles) in the second fatigue stage have little effect on fatigue life and the diffusion of chloride ions [102]. In addition, Ren et al. [47] found there is an exponential relationship between the chloride diffusion coefficient and the stress level of fatigue bending load, as shown in Fig. 15. But, compared with the static load, the chloride diffusion coefficient under fatigue load increases faster. Concerning the effect of axial fatigue tensile loading on chloride ion permeability, Fu et al. [104] found, using a series of tests where the stress level varied from 0.25 to 0.40, that the chloride diffusion coefficient of fatigue-damaged concrete subjected to axial tensile fatigue loading increased by ~ 1.5–3.0 times.

Residual strain is often used as an indicator characterizing the degree of fatigue damage. Saito et al. [97] pointed out that, compared with the stress level and the number of fatigue cycles, there is a good relationship between fatigue residual strain and chloride ion permeability. The degree of fatigue damage can be treated as the ratio of residual strain caused by a fatigue loading with a certain number of cycles and ultimate residual strain, as shown in Eq. (6).

$$P = \frac{\varepsilon_n}{\varepsilon_{\max}} \tag{6}$$

where P is the degree of fatigue damage (%), ε_n is the residual strain after n fatigue cycles loading, and $\varepsilon_{\max}$ is the ultimate residual strain when fatigue failure occurs. Wang [64] carried out chloride diffusion tests on concrete with different degrees of fatigue damage and found

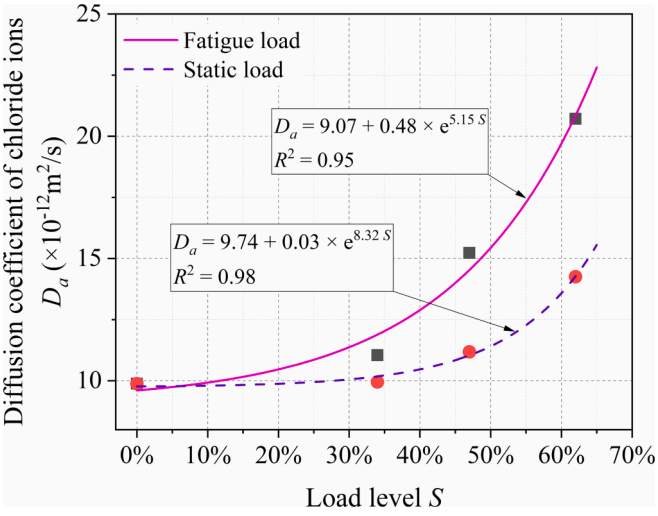

Fig. 15. Relationship between chloride diffusion coefficient and fatigue stress level [47].

that, when the degree of fatigue damage reached 20 %, the chloride diffusion coefficient started to increase. They also found that the chloride electric flux value of concrete with 50 % damage was 2.6 times that of undamaged concrete. Under flexural fatigue loading, the degree of damage in the tension and compression zones is different, and the critical degree of fatigue damage when the chloride diffusion coefficient increases significantly in the two zones becomes 0.4 and 0.6, respectively [105]. The quantitative relationship between fatigue damage and chloride diffusion coefficient is shown in Eq. (7) and Eq. (8).

Bending fatigue tension zone: $D = D_0\left(0.6249 + 0.3557e^{1.3854P}\right)$ (7).

Bending fatigue compression zone: $D = D_0\left(0.9566 + 0.0270e^{3.6069P}\right)$ (8).

where D is the chloride diffusion coefficient of fatigue-damaged concrete, and D_0 is the chloride diffusion coefficient of undamaged concrete. For fatigue-damaged concrete under uniaxial tensile fatigue loads, Fu et al. [104] indicated that the increase in apparent chloride diffusivity was linearly correlated to residual strain.

In recent years, concrete damage detection techniques, such as acoustic emission and electrical impedance spectroscopy, have been gradually applied to fatigue damage detection in concrete. Wang et al. [113] used acoustic emission technology to detect the damage distribution inside a mortar specimen under the coupling action of bending fatigue loading and chloride corrosion in real time. Wang et al. [109] also described the acceleration mechanism of chloride ion permeability in mortar under fatigue loading from a mesoscopic view, showing that adding slag into the cement mortar can effectively improve resistance to chloride ion penetration under fatigue loading. Using the electrical resistance obtained by electrical impedance spectroscopy to characterize the degree of fatigue damage, Song et al. [98] and Jiang et al. [111] evaluated the effect of axial fatigue loading on chloride diffusivity. Under axial compressive fatigue stress, the electrical resistance is linearly negatively correlated with the chloride diffusion coefficient while, under axial tensile fatigue stress, the electrical resistance, like residual tensile strain, has an exponential relationship with the chloride diffusion coefficient.

In summary, current studies on chloride corrosion under fatigue loading mostly focus on bending fatigue loading, and there are few studies of axial compressive and tensile fatigue loading. In addition, methods of quantitative characterization of the degree of fatigue damage of concrete and establishing the relationship between fatigue damage and chloride diffusion performance of concrete are still the focus of ongoing research, for example, by using some advanced damage detection technologies such as acoustic emission.

5.3. Chloride ingress model accounting for fatigue loading

As mentioned above, the diffusion of chloride ions in concrete follows Fick's second law of diffusion. Since Collepardi et al. [88] first applied Fick's second law to build a chloride diffusion model, some modified diffusion models, that allowed for the effects of various factors, have been gradually established. Applying fatigue loads to concrete causes the generation and development of microcracks, accelerating the transmission of chloride ions into the concrete.

Gerard et al. [114] proposed a diffusion model accounting for mechanical loading, as shown in Eq. (9).

$$D(\gamma) = D_0 + D_{\max}\left(1 - \frac{1}{1 + (\gamma/\gamma_{cr})^n}\right) \tag{9}$$

where $D(\gamma)$ is the diffusion coefficient accounting for mechanical damage, γ is the fatigue damage parameter, D_0 is the diffusion coefficient for undamaged concrete, $D_{\max}$ is the diffusion coefficient in completely cracked concrete, and n and γ_{cr} are model parameters. Although this model mainly focuses on the chemical corrosion caused by the leaching of pore solution ions, it can be used as a basis for modelling

Table 4
Chloride ingress models of fatigue-damaged concrete from the literature.

Literature	Year	Model	Annotation for main parameters	Note
Xiang et al. [115]	2007	$\frac{\partial C(x,t)}{\partial t} = D_f(x,t)\frac{\partial^2 C(x,t)}{\partial x^2} + \frac{\partial D_f(x,t)}{\partial x}\frac{\partial C(x,t)}{\partial x}$ $D_f = D_0 + D_{max}\left(1 - \frac{1}{1+(\gamma/0.4)^5}\right)$	$C(x,t)$ = chloride ion concentration at time t at distance × from the concrete surface x = concrete depth t = action time D_f = chloride diffusion coefficient in fatigue-damaged concrete D_0 = chloride diffusion coefficient in undamaged concrete D_{max} = chloride diffusion coefficient in completely damaged concrete γ = fatigue damage parameter	• As a numerical model Chloride diffusion coefficient considering fatigue damage is time and depth dependent
Jiang et al. [116]	2010	$C(x,t) = C_0 + (C_s - C_0)\left(1 - \mathrm{erf}\left(\frac{x}{2\sqrt{D_{af}t}}\right)\right)$ $D_{af} = 3.2 + 0.8\exp(\frac{\varepsilon_n}{45})\varepsilon_n = \left(\frac{5n}{4\times 10^{(a-S_{max})/b}} - \frac{1}{8}\right)\varepsilon_B$	C_0 = initial chloride ion concentration C_s = surface chloride ion concentration erf = an error function D_{af} = apparent chloride diffusion coefficient under fatigue loading ε_n = residual strain after n fatigue cycles n = fatigue loading cycles ε_B = ultimate residual strain a, b = test constants related to materials S_{max} = maximum stress level	• Residual strain as a way of characterizing the fatigue damage
Ren et al. [47]	2015	$C(x,t) = C_s\left(1 - \mathrm{erf}\left(\frac{x}{2\sqrt{D_{af}t}}\right)\right)$ $D_{af} = 9.07 + 0.48\exp(5.15S_{max})$		• Chloride diffusion coefficient accounting for fatigue damage is related to the maximum fatigue stress level
Yang et al. [117]	2019	$C(x,t) = C_0 + (C_s - C_0)\left(1 - \mathrm{erf}\left(\frac{x}{2\sqrt{D_{af}t}}\right)\right)$ $D_{af} = D\left(1 + \frac{D_c\rho_e}{D}\left(\frac{1}{1 - \frac{ft}{10^{(a-Smax)/b}}} - 1\right)\right)$	D = initial chloride diffusion coefficient in concrete D_c = maximum chloride diffusion coefficient of in concrete cracks ρ_e = initial microcrack area density of concrete f = frequency of the fatigue loading	• Diffusion of chloride ions in fatigue damaged concrete is treated as a coupling between diffusion in undamaged concrete and diffusion in cracks Diffusion coefficient varies over duration of action
Wu et al. [107]	2021	$C(x,t) = C_0 + (C_{s,\Delta x} - C_0)\left(1 - \mathrm{erf}\left(\frac{x-\Delta x}{2\sqrt{D_{af}t}}\right)\right)$ $D_{af} = K_{\omega/\gamma}K_T K_{RH} D_m$ $K_\omega = 0.006\exp(0.05\omega) + 0.9874$ (Crack widths dominated) $K_\gamma = 1 + 11.9\left(1 - 1/\left(1 + (\frac{\gamma}{0.4})^5\right)\right)$ (Fatigue damage dominated) $K_T = \exp(0.028(T-23))$ $K_{RH} = \left(1 + (\frac{1-RH}{1-0.75})^4\right)^{-1}$ $\gamma = \frac{F_{max} - F_{min}}{F_u}$ $D_m = \frac{D_{ref}}{1-m}\left(\frac{t_{ref}}{t}\right)^m, t < t_R$ $D_m = D_{ref}\left(\frac{t_{ref}}{t_R}\right)^m\left(1 + \frac{t_R}{t}\left(\frac{m}{1-m}\right)\right), t \geqslant t_R$	$C_{s,\Delta x}$ = chloride ion concentration at the depth of convection zone Δx Δx = depth of convection zone K_ω, K_γ, K_T, K_{RH} = influential factor of fatigue cracks, fatigue damage, temperature, relative humidity D_m = chloride diffusion coefficient on average within time t ω = main crack width T = environment temperature RH = relative humidity F_{max}, F_{min}, F_u = maximum, minimum fatigue load and ultimate load D_{ref} = chloride diffusion coefficient at t_{ref} t_{ref} = reference time t_R = critical time after which the D_m keeps constant m = coefficient related to materials	• This chloride ingress model can be applied to wet-dry cycled environments

chloride diffusion in load-damaged concrete, as shown in Table 4 which summarizes the chloride ingress models of fatigue-damaged concrete in existing literature. Using this model and introducing parameters that describe the damage of compressive fatigue and tensile fatigue, Xiang et al. [115] created a chloride corrosion model for concrete that accounted for the non-uniform distribution of fatigue damage and stress in the concrete section, with fatigue damage parameters as a function of loading time. Therefore, the chloride diffusion coefficient in fatigue-damaged concrete has time and space dependence. However, this model is a numerical model involving complex calculations, and is difficult to use. Wu et al. [107] also established a chloride ingress model based on Eq. (9), allowing for fatigue damage and the effects of ambient temperature and relative humidity. In addition, in this model, the effect of cracks generated by fatigue loading on chloride diffusion are treated separately, so this model is more suitable for the simulation of chloride diffusion in concrete after fatigue damage, where the coupling effect of fatigue loads and chloride corrosion is not accounted for.

The effect of fatigue loading on the diffusion of chloride ions in concrete is because repeated fatigue loading can generate microcracks. Therefore, the diffusion of chloride ions in fatigue-damaged concrete can be treated as a coupling effect between diffusion in the uncracked concrete matrix and in the cracks. Based on this hypothesis, Yang et al. [117] established a time-varying diffusion model of chloride ions accounting for fatigue damage, based on the theoretical equation of concrete fatigue damage, which links material properties, fatigue stress level and loading frequency. However, neither the deterioration of porosity in concrete nor the inhomogeneity of the crack width along the height axis in the flexural-tension zone of the concrete flexural member are considered in this model. In addition, Jiang et al. [116] used the residual strain as an index to measure the degree of fatigue damage. Based on experimental data, the relationship between the apparent chloride diffusion coefficient and residual strain, along with a model for chloride diffusion under fatigue loading, were established. In this model, the development of the residual strain during fatigue loading is kept consistent with the change in the relative cycle life ratio, i.e., the ratio between number of applied numbers of fatigue cycles and fatigue life, it is assumed that the residual strain starts at the second stage of the fatigue damage curve, and the assumption is that the ultimate residual strain is the corresponding residual strain at the end of the second stage. Therefore, the model can directly produce the change in chloride diffusion coefficient according to the number of fatigue loading cycles and the maximum stress level in the actual concrete structure. Ren et al. [47] also determined the relationship between the apparent chloride diffusion coefficient and the maximum fatigue stress level based on experimental data from a coupled test of fatigue loading and chloride corrosion. However, most parameters in these two models are obtained by fitting experimental data, and the applicability of fitting parameters needs to be verified by further experiments.

From the above description, we can see that the existing chloride ingress models that consider fatigue damage still have some shortcomings. During the process of fatigue loading, pore structures inside the concrete continuously deteriorate, and the number, width, and length of microcracks also gradually increase. Therefore, the effect of time-varying fatigue damage on the chloride diffusion cannot be ignored. In addition, the damage to concrete caused by different fatigue loading states is different. The damage to concrete caused by axial compressive fatigue loading and tensile fatigue loading can often be regarded as uniform damage along the section's height or width. However, under bending fatigue loading, the stress distribution of the concrete section is not uniform, resulting in non-uniformity of fatigue damage. Therefore, the chloride diffusion coefficient from the concrete surface to the interior is depth dependent. Better chloride ingress models that account for fatigue damage need to be further studied in the future.

6. Combined effect of fatigue loading and FTCs

6.1. FTC effect on concrete

In a cold environment, the effect of FTCs is one of the main causes of performance degradation of concrete materials and structures. With FTCs, the concrete mainly suffers from physical damage, including cracking, surface peeling, an increase in internal porosity and a decrease in density [118], resulting in a significant reduction in its strength, dynamic elastic modulus and other mechanical properties [7]. Furthermore, this physical damage also exacerbates the transmission of corrosive substances from the external environment [119], such as carbon dioxide, chloride ions, sulphate ions, and moisture, which accelerate the corrosion rate of reinforcement material embedded in the concrete structure, reducing the safety of the structure.

The degree of saturation of the pores inside the concrete is the main factor affecting the frost resistance of concrete. Fagerlund [120] pointed out that only when the degree of saturation reaches a certain critical value can clear freeze–thaw damage in the concrete appear. There has been extensive research into the mechanism of freeze–thaw damage of concrete. Hydraulic pressure theory was first proposed by Powers [121] to explain the damage mechanism of concrete subjected to water FTCs, leading to the discovery that osmotic pressure was the driving force behind frost damage when the concrete was in a freeze–thaw environment with salts [122]. The water frost damage mechanism of the concrete is shown in Fig. 16. Under the negative temperature condition, the temperature gradually decrease from the surface to interior of the concrete, and the pore water on the surface of the concrete is first frozen to form the ice. The volume increase from water to ice in pores leads to the migration of liquid water and the generation of hydraulic pressure. When coupling action of crystallization pressure of ice and hydraulic pressure exceeds the tensile strength of concrete, microcracks will occur [123,124]. However, there is no consensus on the salt frost damage of concrete [125]. In addition to ice crystallization pressure and the

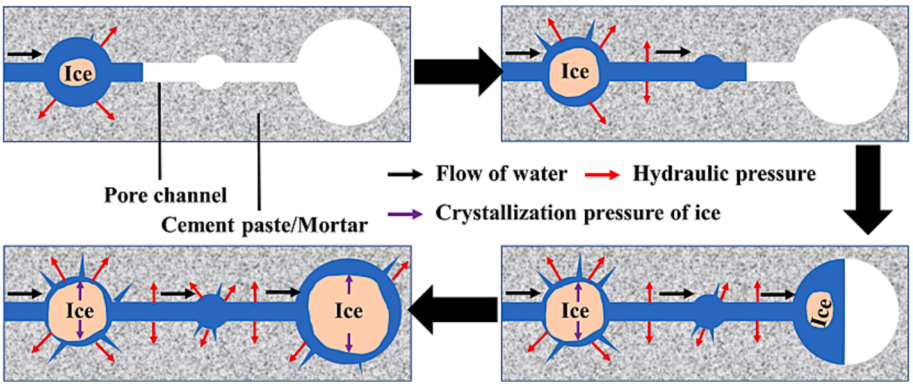

Fig. 16. Hydraulic pressure damage of the concrete in water FTCs.

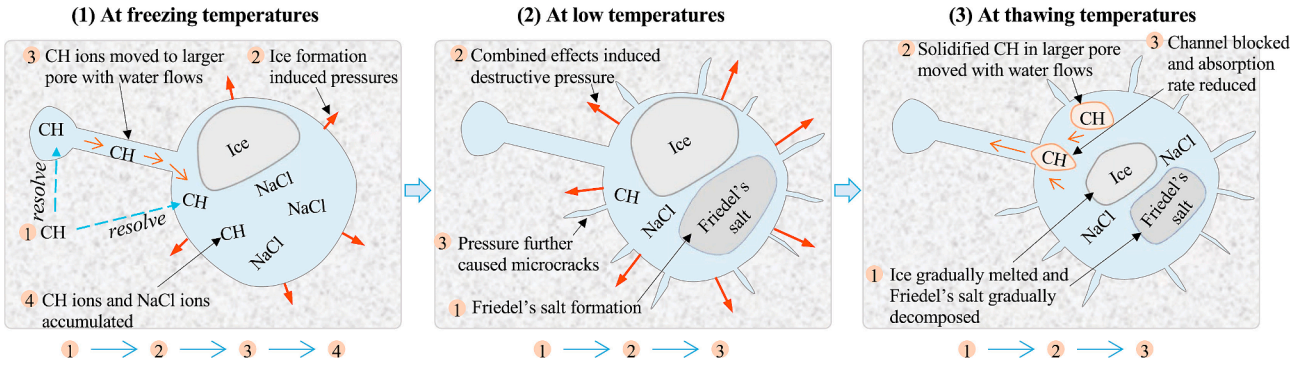

Fig. 17. Frost damage mechanism of the concrete in salt FTCs [128].

generated osmotic pressure caused by the difference in solution concentration between unfrozen and frozen pores, the expansion stress caused by salt crystallization also damage the concrete [128], as shown in Fig. 17. In addition, the forms of damage that concrete undergoes in water freeze–thaw and salt freeze–thaw environments are also different, with the former mainly generating microcracks inside the concrete and the latter mainly causing peeling of the surface matrix [118]. Moreover, the air content inside the concrete is a major factor influencing the frost resistance. Adding an air-entraining agent into concrete can create tiny evenly-distributed pores inside the concrete, which can release the hydrostatic pressure generated by the conversion of water into ice and thus reduce freeze–thaw damage [12].

FTCs are often accompanied by coupling with some chemical attacks, including carbonation, chloride ion attack and sulphate corrosion. These chemical attacks have both positive and negative effects on the resistance to freeze–thaw of concrete. On the one hand, the presence of chloride or sulphate ions can reduce the freezing point of the pore solution in concrete, delaying freeze–thaw damage [126,127], while the carbonate salts formed by carbonation can improve the compactness of concrete which reduces the penetration of external moisture, enhancing frost resistance [3]. However, the beneficial effects of these chemical attacks on resistance to freeze-thawing of concrete mainly occur in the initial stage of FTCs. With extended exposure duration, on the other hand, the crystallization of chloride salts [128], formation of ettringite and gypsum from sulphate corrosion [129], and accumulation of carbonate salts [127], can all generate high crystallization pressures and expansion forces in concrete, coupled with the hydrostatic pressure caused by FTCs, to accelerate the deterioration of concrete.

6.2. *Concrete damage under the combined effects of fatigue loading and FTCs*

In addition to chemical attacks, the combined effect of FTCs and mechanical loading also accelerates the deterioration of concrete and shortens the service life of the structure. This is especially true of concrete structures such as bridges in cold regions, which usually suffer from the combined effect of fatigue loading and FTCs. The damage mechanisms for both FTCs and fatigue loading on concrete are similar,

Table 5
Experimental studies into the concrete under the combined effect of fatigue loading and FTCs.

Literature	Year	Specimen size (mm × mm × mm)	Test methods*	Fatigue loading type	Max. stress level	Loading frequency (Hz)	Condition of FTC action	Fatigue damage index
Forgeron et al. [132]	2004	100 × 100 × 350	FT + F	Four- point flexural	0.4, 0.45		300 cycles	Residual flexural strength, residual flexural stiffness.
Hasan et al. [133]	2008	φ100 × 200	FT + F	Uniaxial compressive	0.6, 0.75	5	0, 50, 100, 300 cycles	Fatigue strength, Fatigue loading cycles
Li et al. [134,135]	2011, 2012	70 × 70 × 280	FFT	Four-point flexural	0.6, 0.65, 0.7, 0.75, 0.8	10	Closed air FTC	Residual strain
Liu et al. [136]	2011	100 × 100 × 515 (PC specimen)	F + FT	Four-point flexural	0.7	5	Rapid water FTC	Number of FTCs
Hong et al. [137]	2012	100 × 100 × 400	FT + F	Four-point flexural	0.556	10	Water/Salt FTC	Fatigue life
Jang et al. [138]	2014	100 × 100 × 400	FT + F	Flexural	0.5 ~ 0.9	1	Rapid water FTC, 150 cycles	Fatigue life
Liu et al. [139]	2015	100 × 150 × 800 (RC specimen)	F + FT	Four-point flexural	0.2, 0.3	5	Rapid water FTC, 300 cycles	Residual strain
Qiao et al. [50,143]	2015, 2018	70 × 70 × 280	FFT	Four-point flexural	0.65	10	Closed air FTC	Strain
Guo et al., [140,141] Yang et al., [142] Shen et al. [51]	2016, 2016, 2018, 2018	100 × 100 × 400	Alternating F + FT	Four-point flexural	0.5, 0.8	10	Rapid water FTC	Pore structure, cracking, strength
Lu et al. [144]	2017	100 × 100 × 300	FT + F F + FT	Uniaxial compressive	0.5	5	Rapid water FTC	Dynamic elastic modulus, strength

(*continued on next page*)

Table 5 (*continued*)

Literature	Year	Specimen size (mm × mm × mm)	Test methods*	Fatigue loading type	Max. stress level	Loading frequency (Hz)	Condition of FTC action	Fatigue damage index
Li et al. [145]	2018	100 × 100 × 400	F + FT	Four-point flexural	0.6, 0.65, 0.7, 0.75, 0.8	10	Rapid water FTC	Strength, dynamic elastic modulus
Boyd et al. [146]	2019	φ100 × 200	FT + F	Uniaxial tensile	0.6, 0.8		0, 25, 50 cycles	Strength, fatigue life
Haghnejad et al. [147]	2021	100 × 100 × 500	FT + F	Three-point flexural	0.6, 0.7, 0.8		Salt FTC	Fatigue life
Yang et al. [148]	2020	100 × 100 × 400 (RC specimen)	FT + F	Four-point flexural	0.65	5	Water/Salt FTC	Residual crack width, dynamic elastic modulus, maximum residual deflection
Zheng et al. [149]	2020	320 × 500 × 2000 (PC specimen)	FT + F	Four-point flexural	0.8	5	50, 75, 100 cycles	Crack development
Chen et al. [150]	2021	100 × 100 × 400	FT + F	Four-point flexural	0.7, 0.75, 0.8, 0.85	5	Rapid water FTC	Fatigue life
Li et al. [151]	2022	100 × 100 × 400	Alternating F + FT	Four-point flexural	0.5, 0.7		Rapid water FTC	Pore structure, dynamic elastic modulus, crack patterns

* In this table, "FT + F" denotes that concrete specimens were first subjected to FTCs and then fatigue loading; "F + FT" denotes that concrete specimens were first subjected to fatigue loading and then FTCs; "FFT" denotes that concrete specimens were subjected to fatigue loading and FTCs simultaneously.

and both can be regarded as the accumulation of internal damage of concrete under repeated action [130]. Although both fatigue loading and FTCs can promote formation and development of microcracks in the concrete, fatigue loading mainly increases the number of cracks, while FTCs cause the propagation of cracks and less tortuous of microcracks [131]. Furthermore, compared with fatigue loading, the alternating frequency of FTCs is much smaller. Therefore, it is not easy to realize a simultaneous coupling test of these two effects. Most existing studies have used an interaction test method to study the combined damage of the two effects, that is, carrying out the fatigue loading test after a certain number of FTCs or carrying out the FTC test after fatigue loading, as shown in the Table 5.

Forgeron et al. [132] found that the residual performance of concrete under the interaction of FTC and fatigue loading is approximately equal to, or even higher than that under a single action and there is no obvious synergistic effect between the two actions. However, most related studies suggested that the combined effect of fatigue loading and FTCs can exacerbate the deterioration of concrete performance. By using flexural fatigue loading on concrete specimens in an environment chamber in which liquid nitrogen was used as a cryogen to produce a closed freeze–thaw environment without water uptake, as shown in Fig. 8, Li et al. [134,135] monitored the damage process of a concrete sample under the coupling effect of fatigue loading and FTCs by using acoustic emission technology. The residual strain of concrete under this coupling action was greater than that under a single action. The main effect of fatigue loading is to produce new microcracks in the matrix and propagate existing cracks which are distributed in the interface transition zone (ITZ) [131,134]. Furthermore, microcracks which are diametrical around the pores and caused by ice forming during FTCs, can bridge between the pores and ITZ, both of which are areas where most damage occurs [134,152]. This indicates that both fatigue loading and FTCs contribute to the damage. In addition, the coupling strains, including the minimum strain and maximum strain as shown the red and blue lines in Fig. 18 respectively, have the property of periodicity, that is, an acceleration period during the freezing stage and an induction period during the thawing stage [50]. During the freezing stage, the formation of ice due to phase transition is the main factor that contributes to crack propagation. Although the degree of coupled damage during the thawing period is lower than for the freezing period, the moisture inside the concrete is redistributed [153], which can quicken the damage in the next freezing period. Considering that, in real life, traffic loads are transient, and the FTCs are also periodic, Guo et al.

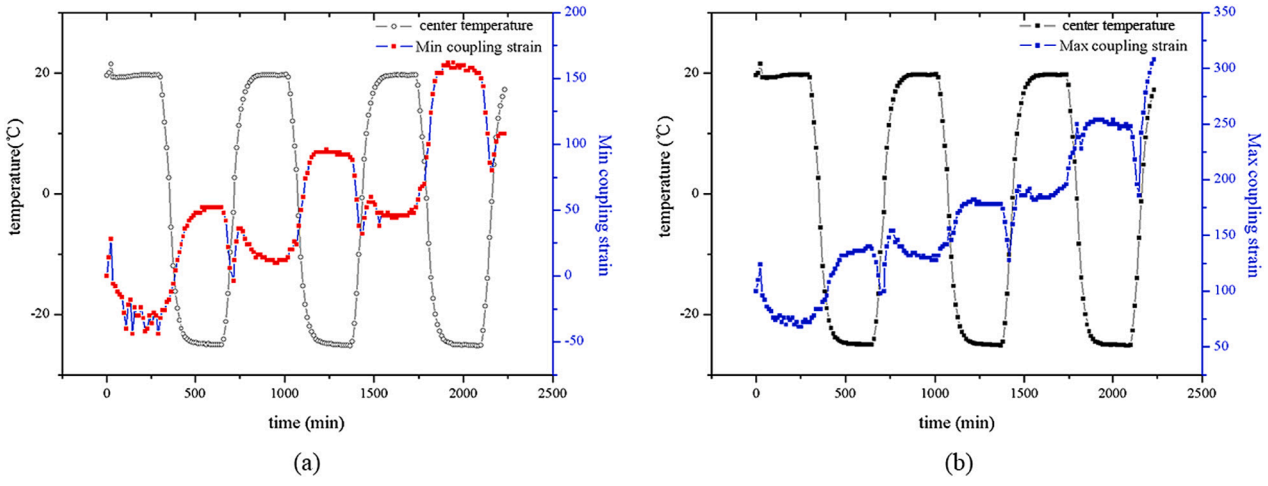

Fig. 18. Coupling strain versus time and temperature (a) minimum strain (b) maximum strain [50].

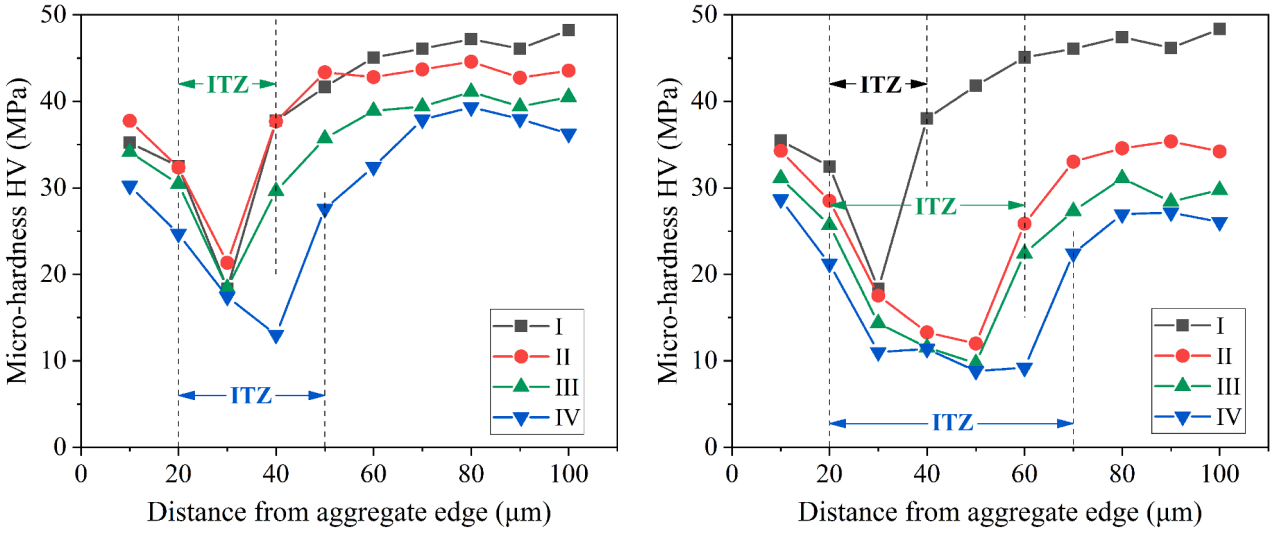

Fig. 19. Microhardness test results for ITZ under fatigue alone and combined action of FTCs and fatigue loading [142] (Here, from I to IV, the action time (fatigue times or combined action cycles) increases)).

[140,141] simulated the combined effect of fatigue loading and FTCs by alternating the two actions multiple times and analysing the damage evolution process from a microscopic perspective. FTCs promote the propagation of cracks but inhibit the widening of the cracks. At the same time, FTCs cause the formation of micropores and edge microcracks, leading to an increase in the fractal dimension of the cracks, that is, an increase in the complexity of the crack distribution [140]. Fatigue loading is the main reason for the deterioration of pore structures inside the concrete, and FTCs can cause significant damage to the pore structure in the later stage of the combined action [141]. Using a microhardness test, as shown in Fig. 19, it was seen that alternating fatigue loading and FTCs deteriorated the ITZ significantly compared with the fatigue loading alone. Its width increased over time, and the deterioration rate was faster than if there was just fatigue loading [142]. It is also demonstrated that there is a coupling damage action between fatigue load and FTCs.

6.3. Concrete properties under the combined effect of fatigue loading and FTCs

Concrete exposed to the combined action of fatigue loading and FTCs suffers more mechanical damage than concrete exposed to just one. Alternating between flexural fatigue loading and FTCs, the flexural strength of concrete exhibits a parabolic decay trend, so the strength decays slowly in the early stage of the alternating actions and decreases quickly in the later stage. There is a good linear correlation between the flexural strength and pore structure parameters of the concrete including the most probable pore diameter, less harmful pores, and specific surface area [51]. Based on the response surface method, Li et al. [145] showed that, under the combined action of FTCs and fatigue loads, the number of fatigue cycles significantly affects the flexural strength of concrete, while the number of FTCs influences compressive strength. However, the related mechanism is not described. How the order of fatigue loading and FTCs affects the compressive properties of concrete has also been studied [144]. For concrete first subjected to compressive fatigue loading and then FTCs, the initial damage caused by fatigue loading can significantly increase the subsequent freeze–thaw damage [133]. For concrete first subjected to FTCs and then fatigue loading, although the initial FTCs produce microcracks, the subsequent compression fatigue loading can compact those cracks and temporarily increase the strength of the concrete [154]. However, with increasing numbers of fatigue cycles and FTCs, the microcracks further develop, resulting in a reduction in strength. In addition, this phenomenon can also be explained by the damage evolution of concrete during fatigue loading or FTCs. Fatigue damage of concrete is a process where the rate of damage occurring accelerates first, then develops smoothly and finally accelerates again [37]. Therefore, the initial damage can increase the amount of subsequent freeze–thaw damage. The amount of freeze–thaw damage in concrete increases slowly and then more quickly, therefore, fewer FTCs do not significantly impact the development of damage. Therefore, the degree of damage of concrete after being subjected to FTCs followed by fatigue loading is lower than that of concrete having been subjected to fatigue loading followed by FTCs. Regardless of the damage modes, with the increase of the number of freeze–thaw cycles and fatigue cycles, the combined effect of fatigue loading and freeze–thaw cycles will cause more serious damage to concrete than the simple sum of any single factor [144]. For concrete experiencing the combined effect of uniaxial tensile fatigue loads and FTCs, fewer FTCs do not significantly affect the ultimate static tensile strength, but considerably deteriorate residual fatigue performance [146]. Yuan et al. [155] also found that FTCs reduce the elastic deformation capacity of concrete, which greatly reduces its fatigue resistance.

Adding appropriate fibres into the concrete can improve the frost resistance and fatigue of concrete, with the addition of 1 % and 3 % polypropylene fibres by mass making freeze–thaw damaged concrete exhibit a high bending fatigue life [147]. Li et al. [151] experimentally discovered that fibre-reinforced concrete with basalt fibres with a similar elastic modulus as aggregate has a higher residual performance than ordinary concrete under the alternating action of fatigue loading and FTCs. With an increase in fatigue stress level, the anti-cracking effect of basalt fibre and the enhancement effect on the frost resistance of concrete are more apparent. Under the same cyclic mechanical loading and FTCs, the residual performance of recycled aggregate concrete is better than that of natural aggregate concrete, and the ITZ of the latter deteriorated significantly faster than that of the former, as measured using microhardness and SEM tests [156]. It can be explained in two ways. Firstly, the high porosity of recycled aggregate can release the ice expansion effect at freezing period. Secondly, the recycled aggregate concrete has an internal curing effect during the freeze–thaw cycle which enhances the microstructure of the concrete by further hydration with the water released by the saturated recycled aggregate [157].

There are currently only a few studies at the component level into reinforced/prestressed concrete structures experiencing a combined action of fatigue loading and FTCs. Liu et al. [158] evaluated the fatigue performance of prestressed concrete beams that had been subjected to FTCs and found that the prestressed tension level and the number of

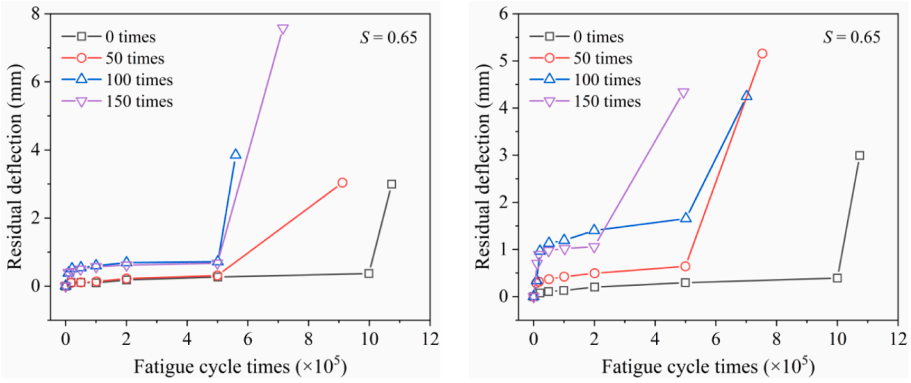

(a) Water FTCs (a) Salt FTCs

Fig. 20. Residual deflection development when subjected to water FTCs or salt FTCs [148] (Here, S = 0.65 means the applied stress level, i.e., the ratio of the maximum fatigue load to ultimate bearing capacity, is 0.65).

FTCs were the main factors affecting fatigue life. FTCs can accelerate the development of member deflection and speed up the point of crack failure of prestressed concrete beams under fatigue loads [149]. For reinforced concrete beams subjected to FTCs, the residual crack width, relative dynamic modulus, residual stiffness, and residual deflection all exhibit obvious three-stage development with a rapid, then slow and finally accelerated failure [148]. As shown in Fig. 20, regardless of water FTCs and salt FTCs, the residual deflection development is similar; whereas with the number of FTCs increases, the salt FTCs condition will advance the failure point of specimen fatigue. The presence of chloride salt can reduce the freezing point of the pore solution to reduce the negative effect of FTCs on fatigue damage in the initial stage [148]. However, because the permeability of salt solution to concrete is much greater than that of water, therefore, with the number of FTCs increases, the saturation degree of concrete increases. The concrete will accelerate deterioration under osmotic pressure and salt crystallization pressure. So, with an increasing number of fatigue cycles, the acceleration effect of salt freeze–thaw on fatigue failure increases.

6.4. *Concrete deterioration models accounting for the interaction of fatigue loading and FTCs*

Freeze-thaw damage occurs when the maximum stress caused by the FTCs somewhere inside the concrete exceeds the tensile strength of the concrete. Damage to concrete caused by repeated FTCs is irreversible and gradually accumulative. The action of FTCs in concrete can be regarded as being fatigue loading with very low loading frequency [130]. Therefore, the classical Aas-Jakobsen fatigue equation [27], as shown in Eq. (1) in Section 2, can also be used to characterize freeze–thaw damage in concrete. The derivation of the freeze–thaw fatigue damage equation for concrete is shown in Fig. 21.

In addition, because fatigue loading can reduce the tensile strength of concrete and then gradually increase the initial stress level S_0, β/S_0 in this equation is related to the number of initial fatigue cycles. Based on this theory, Liu et al. [136] proposed a freeze–thaw deterioration model of concrete accounting for fatigue loads, as shown in Eq. (10).

$$D_n = 1 - \frac{1}{1 - (0.3067 - 0.2365\exp(-0.1088m))\log\left(1 - \frac{n}{N_f}\right)} \tag{10}$$

where m is the number of initial fatigue cycles, n is the number of FTCs, and D is the degree of freeze–thaw damage. Usually, the relative dynamic elastic modulus can be used to reflect the damage inside the concrete caused by FTCs [159], including the formation of microcracks or the coarsening of the pore structure.

Relating to the fatigue life model of freeze–thaw damaged concrete, as shown in Table 6, both Hong et al. [137] and Jong et al. [138] established corresponding models based on the Aas-Jakobsen fatigue equation and introduced a freeze–thaw damage parameter. In addition, regardless of whether the concrete suffers freeze–thaw damage, when the true fatigue stress level is the same, the fatigue life is basically the

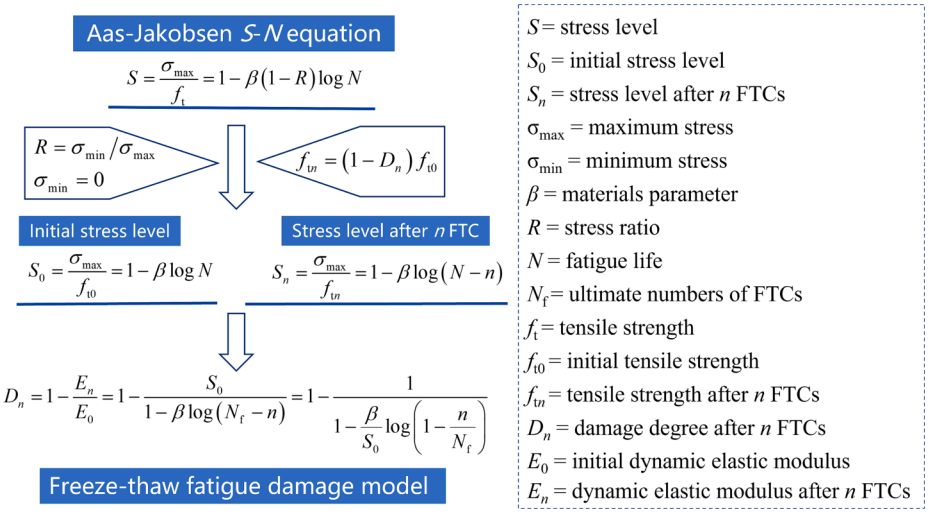

Fig. 21. Derivation of the freeze–thaw fatigue damage model.

Table 6
Fatigue damage model accounting for FTCs.

Literature	Year	Model	Annotation for main parameters	Note
Hong et al. [137]	2012	$S^D_{max} = S_{max}/e^{-D/p} = 1.0 - 0.0572 \cdot \lg N^D_f S^D_{max} = \sigma_{max}/f_{r\text{-}FTD} S_{max} = \sigma_{max}/f_r D = 1 - E_d/E_{d0}$	S_{max} = maximum stress level of undamaged concrete S^D_{max} = maximum stress level of freeze–thaw damaged concrete $f_{r\text{-}FTD}$ = the static flexural strength of freeze–thaw damaged concrete f_r = the static flexural strength of undamaged concrete D = degree of freeze–thaw damage p = fitting coefficient N^D_f = fatigue life of freeze–thaw damaged concrete E_d = dynamic elastic modulus of freeze–thaw damaged concrete E_{d0} = dynamic elastic modulus of undamaged concrete	• Dynamic elastic modulus as the index of degree of freeze–thaw damage
Jang et al. [138]	2014	For Portland cement concrete $S^D_{max} = S_{max}/(f_{r\text{-}FTD}/f_r) = 1.1054 + 0.5650 \cdot \lg(f_{r\text{-}FTD}/f_r) - 0.1365 \cdot \lg N^D_f$ For fibre-reinforced concrete $S^D_{max} = S^D_{max}/(f_{r\text{-}FTD}/f_r) = 1.1717 + 0.5945 \cdot \lg(f_{r\text{-}FTD}/f_r) - 0.1206 \cdot \lg N^D_f$		• Loss of flexural strength as the index of degree of freeze–thaw damage
Liu et al. [158]	2009	$N^D_f = (D_{cr} - D_0)/k_{FTD} k_{PS} k D_0 = 0.2671 \cdot 0.1^{1-0.9418 k_{FTD}} k_{FTD} = 1 - 4.6 \times 10^{-3} m + 8 \times 10^{-5} m^2 - 5 \times 10^{-7} m^3 k_{PS} = 1 - 0.89945 q + 0.6625 q^2$	D_{cr} = degree of critical damage when the concrete experiences fatigue failure, $D_{cr} = 0.34$ in this reference D_0 = degree of initial damage when the fatigue cycle life ratio n/N^D_f is 0.1 k_{FTD} = the effect factor allowing for freeze–thaw action k_{PC} = the effect factor of prestressing stress level k = reduce rate of dynamic elastic modulus, which is obtained by testing n = the number of fatigue cycles m = the number of FTC q = prepressing stress level	• Dynamic elastic modulus as the index of degree of fatigue damage It is assumed that when the fatigue cycle life ratio is larger than 0.1, the degree of fatigue damage is linearly related to the number of fatigue cycles

same [137]. FTCs reduce concrete strength and then increase the true fatigue stress level of the concrete. Liu et al. [158] used the cumulative damage theory to establish a fatigue life equation for prestressed concrete beams with freeze–thaw damage. In this model, the effects of initial FTCs and prestress level on fatigue life were accounted for.

However, some of the parameters in the aforementioned concrete deterioration model for the interaction of fatigue loading and FTCs were obtained by fitting experimental data, and so their applicability needs to be verified further experimentally. In addition, for real life concrete structures, the FTCs and fatigue loading either act simultaneously or alternately on the concrete, whereas the aforementioned models only consider one-time alternating action of the two effects. Further research is needed to study the deterioration process and establish a corresponding damage model of concrete performance after repeated alternating actions of fatigue loading and FTCs.

7. Combined effect of fatigue loading and sulphate corrosion

7.1. Sulphate corrosion of concrete

Sulphate attack on concrete is a complex physicochemical process. Sulphate ions transported from the external corrosive environment to the interior of the concrete can react with cement hydrates such as tricalcium aluminate, and hydration products including calcium monosulfoaluminate (Afm) and calcium hydroxide, to generate expansive products such as ettringite and gypsum [8]. It is worth noting that some sulphate ions are also released to the pore solution due to high temperatures inside the concrete mainly caused by cement hydration, resulting in the generation of ettringite crystallization at ambient temperatures [160]. This process is a delayed ettringite reaction in the form of internal sulphate attack which is different from external sulphate attack. Here, we will mainly focus on external sulphate attack.

Expansive corrosion products, in the initial stage of sulphate attack, can fill the pores and compact the microcracks inside the concrete, improving its compactness and strength [161]. However, once the concentration of expansive products reaches a critical value, the expansion force can exceed the tensile strength of concrete, resulting in the matrix cracking and a loss of strength and stiffness of the concrete [129,162]. Both the water-cement ratio and the composition of cement-based materials significantly affect the resistance to sulphate attack of concrete. Reducing the water-cement ratio of concrete and using cement with a low concentration of tricalcium aluminate is an effective way to improve sulphate attack resistance [163]. In addition, the corrosive environmental conditions are also the main factors affecting sulphate corrosion of concrete. When there is a high concentration of sulphate salt, gypsum is the main expansive product, because ettringite is not stable and decomposes to gypsum when the pH value of pore water falls below about 11.5 [164]. The presence of magnesium ions can convert the C—S—H gel into M—S—H without cohesive force, especially in corrosion by magnesium sulphate solution, thereby loosening the structure and reducing its strength [165,166].

There have been extensive studies of the expansion mechanism and

performance deterioration of concrete subjected to sulphate attack. However, concrete structures are constantly subjected to the action of various loads over their lifetime. Under mechanical loading, unlike the unstressed state, the cracks created by loading can accelerate sulphate attack. In turn, the physical damage caused by sulphate attack to concrete can also affect its bearing capacity [167]. Under the action of static compressive loading, the degree of sulphate attack is related to the applied compressive stress level. A compressive level below about 0.275 can slow down the process of sulphate attack by compacting the microcracks and pore inside the concrete, while a compressive level greater than 0.65 can accelerate the sulphate attack significantly due to generation of more cracks caused by high stress [168]. For tensile stress, sulphate attack is accelerated regardless of the stress level [167].

7.2. Concrete properties under the combined effect of fatigue loading and sulphate corrosion

In addition to being subjected to static loading, some reinforced concrete structures, such as bridges, are often subjected to fatigue loading caused by vehicles, trains, or wind. Compared with static loading, there are limited studies on concrete under the combined action of fatigue loading and sulphate corrosion. A summary of relevant research is shown in Table 7.

Using the experimental setup shown in Fig. 7, the mechanical properties of concrete under simultaneous bending fatigue loading and sulphate attack were investigated [48]. Sulphate attack of concrete is mainly divided into two stages. As shown in Fig. 22, in the first stage, due to the formation of expansive products such as ettringite and gypsum, the compactness of the concrete increases, resulting in an increase in its strength [161]. In the second stage, the crystallization pressure of ettringite and gypsum increases as corrosion continues and then causes the generation of microcracks inside the concrete, resulting in a gradual decrease in its strength [162]. However, under the combined action of fatigue loading and sulphate attack, the phenomenon where formation of expansion products increases concrete strength weakens and even disappears at the initial stage [48]. As shown in Fig. 23, when the fatigue stress level is 0.6, the concrete strength decreases continuously with the increase of corrosion time. This is because the reinforcement effect on concrete strength given by the formation of expansion products is offset by the fatigue damage. A higher sulphate concentration makes the compensation effect of sulphate corrosion on the strength of concrete at the initial state and the deterioration effect at later stages more noticeable [48] i.e., the strength of concrete at the initial corrosion stage with 10 % sulphate concentration is slightly higher than that with 5 % sulphate concentration. In the later stages of corrosion, 10 % sulphate concentration makes concrete strength deteriorate more rapidly than with 5 % sulphate concentration. Based on this, Yu et al. [48] described the degradation process of concrete under sulphate attack alone and under coupled action with fatigue loading, as shown in Fig. 22. The difference with sulphate attack alone is that, under the coupling action, the expansion and cracking stage begins immediately after sulphate ion diffusion occurs. In addition to the fact that fatigue loading can cause earlier cracking of the concrete and thus make it easier for sulphate ions to enter the interior of concrete earlier, a high stress level can also accelerate chemical reactions in the pore solution [173], thereby accelerating the expansion damage by sulphate attack. The addition of mineral admixtures, such as low calcium fly ash, can improve the corrosion fatigue resistance of concrete [162], because the pozzolanic reaction of fly ash can consume lime [174], thereby reducing the amount of gypsum formed by the chemical reaction between sulphate ions and lime. In addition, the partial replacement of cement with fly ash can reduce the content of tricalcium aluminate [175], thereby weakening the reaction between tricalcium aluminate and gypsum. However, incorporating high concentrations of calcium fly ash makes the concrete more susceptible to sulphate attack due to the generation of calcium aluminate hydrates and monosulfate [176]. In addition, concrete structures in tidal zones often suffer from sulphate corrosion due to wetting–drying action, rather than due to being fully underwater. Compared with full immersion, the concentration gradient inside and outside the concrete under wetting–drying cycles can accelerate the transmission of sulphate ions to the interior of the concrete, exacerbating the fatigue corrosion of the concrete [162].

By subjecting concrete first to fatigue loading and then sulphate corrosion, Yan et al. [171] investigated the effect of steam curing on fatigue resistance and corrosion, and found that, compared with standard curing, the fatigue-damaged steam cured concrete lost more strength during sulphate attack. They suggested that compressive fatigue loading with a stress level of 0.5 was sufficient to cause compression cracking and then to accelerate sulphate attack. In addition, the concrete containing slag had lower fatigue resistance and larger strength reduction than that of concrete without slag after the combined action of fatigue loading and sulphate attack. Investigating the influence of sulphate corrosion on the fatigue performance of concrete, both Long et al. [170] and Ting et al. [172] evaluated the fatigue behaviour of concrete by first carrying out the sulphate attack test and then fatigue loading, as shown in Fig. 24. Compared with the uncorroded concrete, the fatigue life of sulphate-corroded concrete is significant lower under the same fatigue load level. This is because that sulphate attack causes severe damage inside the concrete and increases the actual fatigue stress level, resulting in a reduction of fatigue life. Carrying out the alternating

Table 7
Experimental studies into concrete under the combined effect of fatigue loading and sulphate attack.

Literature	Year	Specimen size (mm)	Test methods*	Fatigue loading type	Max. stress level	Loading frequency (Hz)	Condition of sulphate attack	Damage index
Zhao et al. [169]	2014	100 × 100 × 400	FS	Four-point flexural	0.6		Immersion, 5 % or 10 % magnesium sulphate solution	Flexural strength, relative dynamic modulus
Yu et al. [48]	2016	100 × 100 × 400	FS	Four-point flexural	0.2, 0.4, 0.6		Immersion, 5 % or 10 % Na_2SO_4 solution	Flexural strength, relative dynamic modulus
Long et al. [170]	2018	100 × 100 × 400	S + F	Four-point flexural	0.6, 0.7, 0.8	10	Mixed sulphate solution	Fatigue life
Yan et al. [171]	2019	100 × 100 × 300	F + S	Uniaxial compressive	0.5, 0.6, 0.7	5	Immersion, 5 % Na_2SO_4 solution	Relative dynamic modulus
Liu et al. [162]	2020	100 × 100 × 400	FS	Four-point flexural	0.2, 0.35, 0.5		Drying-wetting cycles, 10 % Na_2SO_4 solution	Mass loss, relative dynamic modulus
Zhang et al. [53]	2021	φ50 × 100	Altered F + S	Uniaxial compressive	0.6		Drying-wetting cycles, 5 %, 10 % or 15 % Na_2SO_4 solution	Residual deformation, elastic modulus
Ting et al. [172]	2021	50 × 50 × 50	S + F	Uniaxial compressive	0.3, 0.4, 0.45, 0.8, 0.85, 0.9	0.6, 0.8, 1.0	Drying-wetting cycles, 5 % or 20 % Na_2SO_4 solution	Fatigue life, residual strain, strength

* In this table, "S + F" denotes that concrete specimens were first subjected to sulphate attack and then fatigue loading; "F + S" denotes that concrete specimens were first subjected to fatigue loading and then sulphate attack; "FS" denotes that concrete specimens were subjected to fatigue loading and sulphate attack simultaneously.

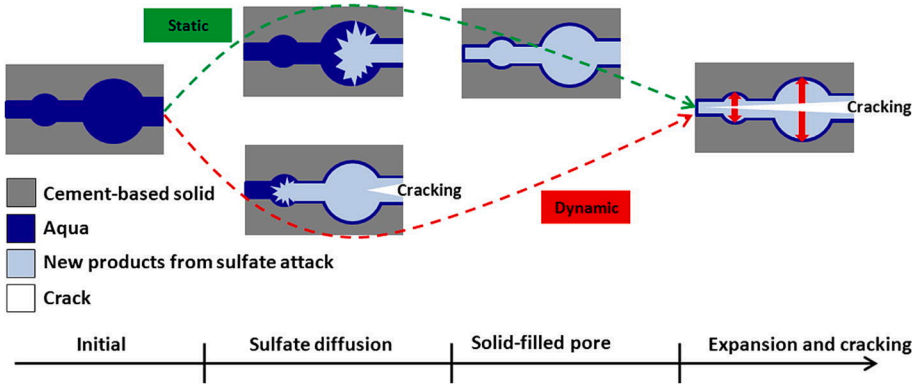

Fig. 22. Damage process of concrete under sulphate attack alone and under the combined action of fatigue loading and sulphate attack [48].

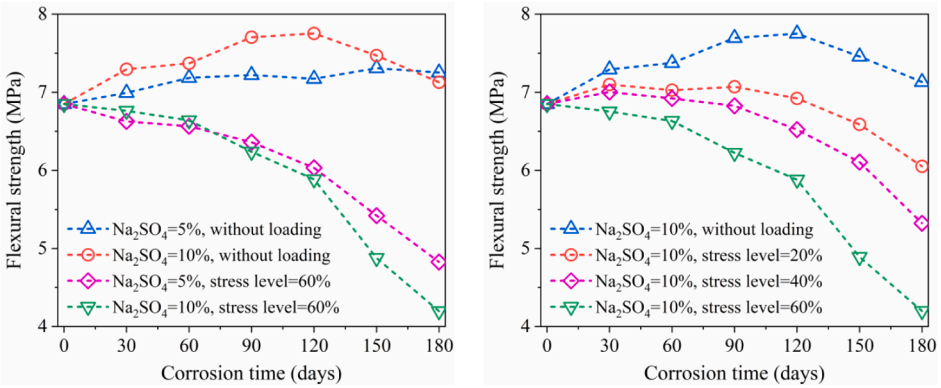

(a) With Na_2SO_4 concentration (b) With fatigue stress level

Fig. 23. Flexural strength of concrete under fatigue loading and sulphate attack with different Na_2SO_4 concentration or fatigue stress level [48].

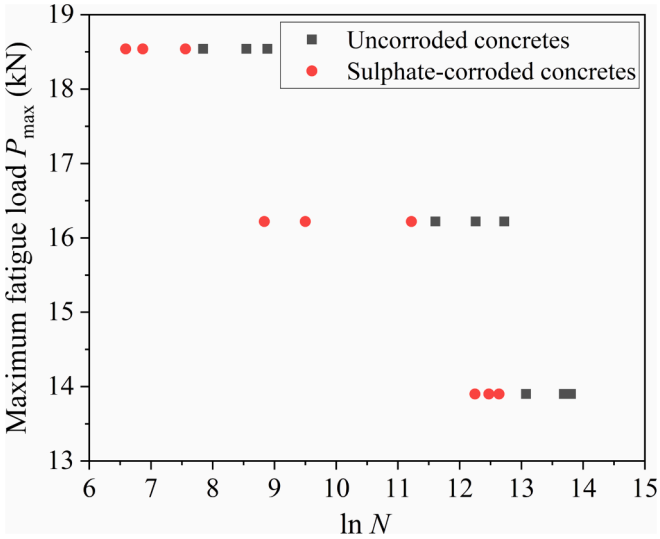

Fig. 24. Maximum fatigue load P_{max}-ln N (N is the fatigue life) curves for uncorroded and sulphate-corroded concretes [170].

test of fatigue loading and sulphate attack in the laboratory can also simulate the actual real-world conditions of concrete. Using 120 cycles of cyclic loading and five wetting–drying cycles of sulphate attack as a major cycle, Zhang et al. [53] evaluated the fatigue behaviour of concrete under the combined effect of fatigue loading and sulphate corrosion. As the number of major cycles increased, the fatigue properties first increased and then decreased. The number of major cycles has a more significant influence on the fatigue behaviour of concrete than does the concentration of sulphate salt.

7.3. Deterioration models that account for the interaction between fatigue loading and sulphate corrosion

There are few studies into models of concrete deterioration under the combined effect of fatigue loading and sulphate attack. Guan et al. [177] treated the transmission of sulphate ions in concrete as a coupling between the transmission in the concrete matrix and that in cracks and established the relationship between the crack factor and the residual deformation during fatigue loading. Finally, they deduced the equation that describes the diffusion coefficient of sulphate ions in fatigue-damaged concrete, as shown in Table 8. On this basis, the sulphate corrosion life model under fatigue loading is established by taking the reaction time when the substances in concrete that can chemically react with sulphate ions are completely consumed as the sulphate corrosion life [177].

However, the aforementioned sulphate ion diffusion coefficient and corrosion life models do not consider the effect of expansion damage due to sulphate corrosion. Compared with chloride ions and carbon dioxide, the transmission of sulphate ions inside the concrete is more complex. In the early stages of corrosion, sulphate attack generates some expansive products such as ettringite and gypsum inside the concrete which fill the internal pores and cracks [161], effectively reducing the transmission of sulphate ions and the diffusion coefficient of sulphate ions. However, with an increase in corrosion duration, the expansion force caused by sulphate attack can cause internal damage to the concrete [162], which accelerates the transmission of external sulphate ions, that is, the

Table 8
Deterioration model under the combined effect of fatigue loading and sulphate attack.

Literature	Year	Model	Annotation for main parameters	Note
Guan et al. [177]	2012	Corrosion-fatigue numerical model: $\frac{\partial U}{\partial t}=\frac{\partial}{\partial x}\left[D_t(x,\ t)\frac{\partial U}{\partial x}\right]-kUC$ $\frac{\partial C}{\partial t}=-\frac{kUC}{\lambda}$ $D_t=D_m+24\times 0.785 n_h \varepsilon_B^P (D_c-D_m)$ $\times 1/\left(24 n_h \varepsilon_B^P+2\times 0.9\times 10^{(S-\alpha)/\beta(1-\nu)}\right)$ Fatigue-corrosion life model: $T=2.2459f+31.563S-0.0014161f^2$ $-0.01564f\cdot S+0.02354f\cdot U_E$ $-5.0734f\cdot w/c-0.31066S^2$ $-0.032872S\cdot U_E-0.080207U_E^2$	U = concentration of sulphate ions x, t = depth and time of corrosion D_t, D_m, and D_c = diffusion coefficients of sulphate ions in the fatigue-damaged concrete, concrete matrix, and cracks. k = constant of reaction rate of sulphate ions C = concentration of calcium ion in the pore solution λ = coefficient of reaction of gypsum n_h = number of fatigue cycles per hour ε_B^P = ultimate residual strain during fatigue loading S = maximum stress level during fatigue loading α, β = test constants related to materials ν = stress ratio of fatigue loading T = fatigue-corrosion life of concrete f = frequency of fatigue loading U_E = concentration of external sulphate ions w/c = water-cement ratio	• The residual strain at the end of the second stage of the fatigue damage process is the same as the ultimate residual strain The diffusion coefficient of sulphate ions in the concrete matrix is related to the porosity of the concrete, water-cement ratio, the degree of hydration, and so on Reaction time when the substances in concrete that can chemically react with sulphate ions are completely consumed is defined as the sulphate corrosion life
Long et al. [170]	2018	Fatigue model accounting for sulphate corrosion: $S=\frac{P_{max}}{D_s P_u}=1.09935-0.08106\lg N_s$	P_{max} = maximum load maximum load D_s = strength degradation factor after sulphate corrosion P_u = static flexural load of uncorroded concrete N_s = fatigue life of the sulphate-corroded concrete	• Loss of static strength after sulphate corrosion is the same as the damage index to characterize the damage caused by sulphate attack

diffusion coefficient of sulphate ions increases. When coupled with fatigue loads, the transmission and damage process during sulphate corrosion is more complex still. Therefore, a method to measure the effects of sulphate corrosion damage and fatigue damage on sulphate ion diffusion simultaneously is the focus of future research. In addition, Long et al. [170] found that the fatigue life of concrete corroded by sulphate attack can be described using the two-parameter Weibull distribution function and obtained the fatigue life model of concrete after sulphate corrosion based on experimental data, as shown in Table 8. However, the experimental data used in the model establishment were limited, and the application of model needs further verification.

8. Discussion and research perspectives

Over the past decade, there has been a good deal of interest in the combined effect of fatigue loading and corrosive environments on the performance of concrete materials or structures. From a concrete material perspective, extant studies on this topic mainly include the effect of fatigue loading on concrete carbonation and chloride transmission, and the damage to concrete under the combined effect of fatigue loading and FTCs or sulphate attack. In addition, some models for carbonation and chloride ingress which incorporate the effect of fatigue loading, along with freeze–thaw damage models, sulphate corrosion models and fatigue life models that include environmental factors have also been created. However, there are still some directions for further exploration and research on this topic.

(1) Most current research about concrete under the combined action of fatigue loading and a corrosive environment uses the one-time alternation simulation test method. In real life applications, however, fatigue loading and corrosion occur simultaneously. Taking the combined action of fatigue loading and carbonation as an example, the damage process for concrete under these actions combined can be divided into the following phases. In the initial stage, low-cycle fatigue loading does not cause significant damage to the concrete, and the carbonation process can be regarded as unaffected by fatigue loading. With an increase in the number of fatigue loading cycles, the damage to the concrete increases with the resulting deterioration of micropores and microcracks significantly accelerating the carbonation process, that is, speeding up the diffusion of carbon dioxide. Furthermore, this damage is time dependent, and therefore, causes the diffusion coefficient of carbon dioxide to become time-dependent also. At the structural level, accelerated carbonation due to fatigue damage can cause the corrosion of reinforcement embedded in the concrete to worsen. Rust will reduce the cross-section of reinforcement material and then reduce the fatigue resistance. Therefore, the reinforcement will deteriorate faster under the combined effect of fatigue loading and corrosion, thereby significantly shortening the service life of the reinforced concrete structure. Therefore, considering the aforementioned deterioration process in concrete structures, it is very important to determine the threshold of the degree of fatigue damage that significantly accelerates the deterioration in concrete durability. Advanced testing techniques should be used in future research to determine, quantitatively and accurately, the degree of damage caused by fatigue loading, such as the change in pore structure, crack width, crack length and distribution of cracks. This can help produce a comprehensive quantitative index to link the damage index and durability indexes, such as the carbonization or chloride diffusion coefficient, and to establish a more accurate durability model that incorporates fatigue damage.

When simulating the combined effect of fatigue loading and corrosion, the best test method is to carry out the fatigue loading and corrosion test simultaneously. However, as mentioned earlier, this test method is complicated to design and operate. A simultaneous test of fatigue loading and chloride or sulphate salt immersion is relatively easy to implement and can be achieved by combining the fatigue loading machine with an immersion tank. However, this test method is difficult to realize when measuring the coupling action of FTCs or carbonation and fatigue loading. In the laboratory, the fatigue loading frequency is generally 5–10 Hz, with the rapid FTC test generally taking 3–4 h for one FTC. Therefore, how to match these two actions is an important issue. Although there are existing test devices that can carry out fatigue loading and FTCs simultaneously, the freeze–thaw environment is a closed air FTCs and does not allow for the transmission of moisture into the concrete [49,50]. In real-world conditions, however, the most serious freeze–thaw damage seen in concrete is often in an environment where there is moisture or salt solution. Therefore, it is very difficult to incorporate moisture or a salt solution in a fatigue loading and FTC

testing environment with large temperature changes. For the carbonation test, because the corrosive medium is carbon dioxide gas, it is also difficult to ensure a constant concentration of carbon dioxide, ambient humidity or temperature in the carbonation box when combined with the fatigue loading machine. An artificial climate simulation room is a good choice to realize the simultaneous test of fatigue loading and corrosion [178], but the influence of temperature change on the fatigue loading and other test equipment needs to be considered; the cost of such testing is also high. Another method that can experimentally simulate the combined effect of fatigue loading and corrosion is a multiple alternated simulation test, as mentioned in Section 3, but current related research is limited. This test method may be considered for future research to simulate the combined action of fatigue loading and corrosion, to determine a reasonable alternating process which can match the real-world conditions of concrete structures.

(2) The type of fatigue loading has a significant effect on the durability of concrete. For concrete subjected to axial compressive/tension fatigue loading, the internal fatigue damage can be regarded as uniform, while the damage caused by flexural fatigue loading is not uniform for concrete beams and other flexural members. Since the tensile strength of concrete is much lower than its compressive strength, the fatigue damage in the tension zone is the most serious. In addition, along the height axis, the damage to the pore structure produced by fatigue loading is not uniform, and the width of cracks is also gradually reduced. Taking the coupling effect of fatigue loading and chloride attack as an example, fatigue damage with uneven spatial distribution will cause inhomogeneity of the chloride ion diffusion coefficient along the depth axis. Considering the time dependence of fatigue damage, the chloride diffusion coefficient has both time and depth dependency under bending fatigue loading. Therefore, the spatial distribution inhomogeneity of fatigue damage should be further investigated in future studies and its impact on durability should be assessed.

(3) Based on the accelerated effect of fatigue damage on the diffusion of chloride ion or carbon dioxide diffusion, some numerical models of chloride diffusion or carbonation allowing for fatigue loading have been created by existing studies, which treat the diffusion flux of chloride ions or carbon dioxide under fatigue loading as a coupling of the diffusion flux between the concrete matrix and fatigue cracks. However, fatigue loading not only causes the development of cracks, but also damages the pore structure of concrete. The effect of the deterioration of the microscopic pore structure caused by fatigue loading on the durability of concrete should also be studied in the future. In recent years, numerical models of concrete with random aggregates have been gradually developed, and the transmission process of chloride ions or carbon

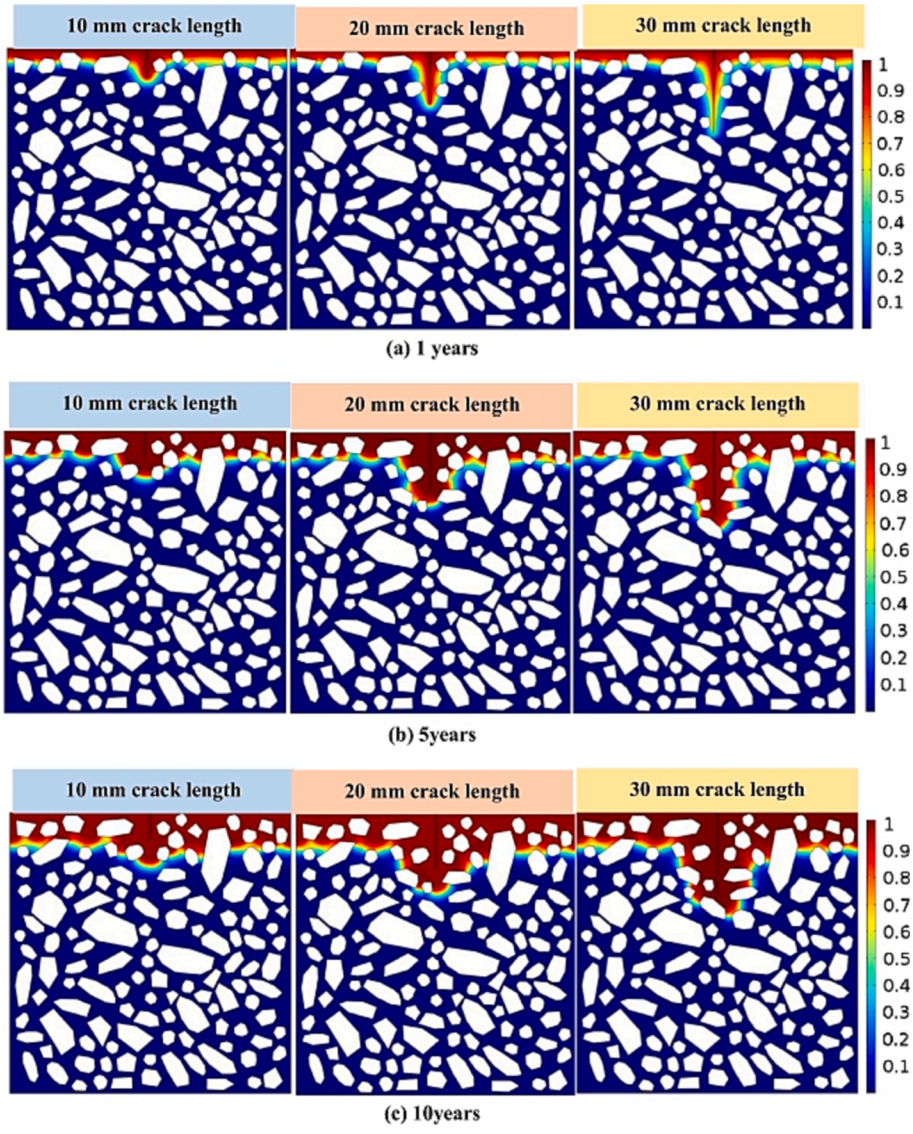

Fig. 25. Relative carbonate content in a numerical model of concrete after carbonation for 1, 5, 10 years [179].

dioxide in concrete has also been simulated [179–181], including numerical models that account for the existence of cracks. One such model is shown in Fig. 25. Compared with static loading, fatigue loading produces more cracks and wider crack distribution in concrete. How to treat fatigue cracks in numerical models of concrete and to simulate the transmission of chloride ions or carbon dioxide are subjects for future research.

For simulation of the coupling between fatigue loading and FTCs, Li et al. [49] proposed an interactive model based on the relationship between the fatigue crack width and permeability coefficient, by combining ABAQUS and HYDRUS-2D finite element software. The propagation of fatigue cracks is simulated and calculated by using the cohesive element in ABAQUS, then the relationship between the cracking and water permeability coefficient is used to calculate the water saturation distribution near the fatigue cracks in HYDRUS-2D. Finally, the degree of local freeze–thaw damage near the cracking is obtained using the relationship between degree of saturation and freeze–thaw damage. However, the inhomogeneity of concrete material has not been incorporated in this model, and the simulation of freeze–thaw cycles to the concrete has not been adequately realized. Qin [182] established a mesoscopic concrete model with random pores and applied radial displacement loading to the pores using the ABAQUS system to simulate freeze–thaw damage at the mesoscopic level. The restart analysis technique is used to simulate the compression of concrete after freeze–thaw damage, and the strength loss obtained agrees with test results [124]. Based on this simulation method, microcracks and coarsened pore structures caused by fatigue loading can be incorporated. Restart technology can also be used to alternately carry out fatigue loading simulation and freeze–thaw damage simulation using a numerical model of concrete, which is a way to realize the numerical simulation of the coupled action of FTCs and fatigue loading. However, whether the restart technique can realize the alternate simulation of fatigue loading and freeze–thaw damage, and how to model the mesoscopic level freeze–thaw damage in the cracked area using a finite element model, both need further research.

(4) There are many corrosive environmental factors that concrete structures suffer from in real-world applications, and often there is more than one at work. Common pairs of such factors include a combination of carbonation and chloride ions, of chloride ions and FTCs, or of chloride attack and sulphate attack. There needs to be more research into the performance degradation of concrete structures under the combined effect of multiple environmental factors and fatigue loading. In addition, there needs to be more research into the performance improvement of concrete under the combined action of fatigue loading and corrosion, for example, the improvement given by the use of fibres on the anti-cracking performance of concrete [183], and the improvement of supplementary cementitious materials on concrete compactness [184].

9. Conclusions

Studies of the performance deterioration of concrete under the combined effect of fatigue loading and corrosive environment factors in the extant literature were reviewed for this paper. From the concrete material perspective, the effect of fatigue loading on carbonation and chloride attack in concrete was described. The deterioration characteristics of concrete under the combined action of fatigue loading and FTCs or sulphate attack were also reviewed. In addition, some carbonation and chloride ingress models accounting for fatigue loading, and damage models of concrete under the combined action of fatigue loading and FTCs or sulphate attack were detailed. The main conclusions drawn from this literature review are as follows:

(1) Due to the complexity of operating and controlling fatigue loading simulation test equipment, it is not easy to carry out a simultaneous test of fatigue loading and corrosion in concrete specimens, especially experiments of the coupling of carbonation or FTCs, and fatigue loading. Most current research used the one-time alternating test method, that is, carried out durability tests after fatigue loading or carried out fatigue loading after exposure to corrosive environments. However, this test method is quite different from the real-world environment of concrete structures. A multiple alternated experiment, that is, where fatigue loading and corrosion are alternately carried out many times, is a potential and controllable test method to simulate the coupling effect of fatigue loads and corrosion on concrete.

(2) Compared with static loading, the deterioration in the durability of concrete under fatigue loading is more severe. Microcracks and coarsened pore structure induced by fatigue loading can accelerate the transmission of corrosive substances from the external environment to the interior of the concrete, resulting in the exacerbation of the degree of carbonation, chloride salt corrosion and freeze–thaw damage. A low compressive stress level can inhibit the transmission of external corrosive substances, while the transmission rate significantly accelerates with an increase in fatigue tensile stress level. Under flexural fatigue loading, the durability deterioration of concrete in the tensile zone is more serious than that in the compression zone.

(3) Fatigue loading and FTCs combine and damage concrete. The cracks generated by the two actions not only develop around the ITZ, but also tend to distribute diametrically around the pores. Coupling damage from the two actions mainly occurs during the freezing phase, with the redistribution of moisture caused by the thawing phase worsening the damage caused by the next freezing phase. Fatigue damage can weaken or offset the increase in concrete strength due to sulphate attack in the initial stage of corrosion, resulting in a gradual decline in strength with an increase in fatigue-corrosion duration. The damage produced by FTCs and sulphate attack increases the true stress level of concrete under fatigue loading and significantly reduces the fatigue life.

(4) The total transmission flux of gases or ions in the fatigue-damaged concrete can be considered as the coupling between the transmission flux in the uncracked concrete matrix and in fatigue cracks. Based on this hypothesis, some carbonation models, chloride ion ingress models and sulphate corrosion models accounting for fatigue damage have been created, in which residual strain is a commonly used indicator that characterizes fatigue damage and can be quantitatively related to the durability indicators of concrete, such as the diffusion coefficients of carbon dioxide, chloride ions and sulphate ions. However, the effect of damage to micropores caused by fatigue loading on the accelerated deterioration of durability cannot be ignored. In addition, the assumption in most models that the transport of external corrosive substances occurs after fatigue damage, is not actually true in real life. Further research is also required into the time-dependence of fatigue damage with loading cycles causing time dependence in the transmission rate of corrosive substances.

Declaration of Competing Interest

The authors declare that they have no known competing financial interests or personal relationships that could have appeared to influence the work reported in this paper.

Data availability

No data was used for the research described in the article.

Acknowledgement

This study was financially supported by the Swedish Transport Administration (Trafikverket) via “Excellence Area 4” and FOI-BBT program (grant number BBT-2019-022).

References

[1] A.M. Neville, Properties of concrete, Fifth Edition, Longman, London, 2011.
[2] Mindess, S., Young, F., & Darwin, D. (2003). Concrete, 2nd edition. Technical Documents, 585.
[3] M.F. Bertos, S.J.R. Simons, C.D. Hills, P.J. Carey, A review of accelerated carbonation technology in the treatment of cement-based materials and sequestration of CO_2, Journal of Hazardous Materials 112 (3) (2004) 193–205.
[4] Q. Qiu, A state-of-the-art review on the carbonation process in cementitious materials: Fundamentals and characterization techniques, Construction and Building Materials 247 (2020) 118503.
[5] M.K. Kassir, M. Ghosn, Chloride-induced corrosion of reinforced concrete bridge decks, Cement and Concrete Research 32 (1) (2002) 139–143.
[6] S.W. Pack, M.S. Jung, H.W. Song, S.H. Kim, K.Y. Ann, Prediction of time dependent chloride transport in concrete structures exposed to a marine environment, Cement and Concrete Research 40 (2) (2010) 302–312.
[7] S. Zhang, B. Zhao, Research on the performance of concrete materials under the condition of freeze-thaw cycles, European Journal of Environmental and Civil Engineering 17 (9) (2013) 860–871.
[8] W. Müllauer, R.E. Beddoe, D. Heinz, Sulphate attack expansion mechanisms, Cement and Concrete Research 52 (2013) 208–215.
[9] A.K. Suryavanshi, R.N. Swamy, Stability of Friedel's salt in carbonated concrete structural elements, Cement and Concrete Research 26 (5) (1996) 729–741.
[10] J. Liu, Q. Qiu, X. Chen, F. Xing, N. Han, Y. He, Y. Ma, Understanding the interacted mechanism between carbonation and chloride aerosol attack in ordinary Portland cement concrete, Cement and Concrete Research 95 (2017) 217–225.
[11] M. Maes, N. De Belie, Resistance of concrete and mortar against combined attack of chloride and sodium sulphate, Cement and Concrete Composites 53 (2014) 59–72.
[12] R. Wang, Q. Zhang, Y. Li, Deterioration of concrete under the coupling effects of freeze–thaw cycles and other actions: a review, Construction and Building Materials 319 (2022) 126045.
[13] R. Mu, C. Miao, X. Luo, W. Sun, Interaction between loading, freeze–thaw cycles, and chloride salt attack of concrete with and without steel fibre reinforcement, Cement and Concrete Research 32 (7) (2002) 1061–1066.
[14] X.H. Wang, D.V. Val, L. Zheng, M.R. Jones, Influence of loading and cracks on carbonation of RC elements made of different concrete types, Construction and Building Materials 164 (2018) 12–28.
[15] N. Banthia, A. Bhargava, Permeability of stressed concrete and role of fibre reinforcement, ACI Materials Journal 104 (1) (2007) 70.
[16] D.H. Kim, K. Shimura, T. Horiguchi, Effect of tensile loading on chloride penetration of concrete mixed with granulated blast furnace slag, Journal of Advanced Concrete Technology 8 (1) (2010) 27–34.
[17] R. Francois, J.C. Maso, Effect of damage in reinforced concrete on carbonation or chloride penetration, Cement and Concrete Research 18 (6) (1988) 961–970.
[18] N. Gowripalan, V. Sirivivatnanon, C.C. Lim, Chloride diffusivity of concrete cracked in flexure, Cement and Concrete Research 30 (5) (2000) 725–730.
[19] H. Horii, H.C. Shin, T.M. Pallewatta, Mechanism of fatigue crack growth in concrete, Cement and Concrete Composites 14 (2) (1992) 83–89.
[20] M.A. Vicente, D.C. González, J. Mínguez, M.A. Tarifa, G. Ruiz, R. Hindi, Influence of the pore morphology of high strength concrete on its fatigue life, International Journal of Fatigue 112 (2018) 106–116.
[21] L. Elfgren, Fatigue capacity of concrete structures: assessment of railway bridges, Luleå University of Technology, Luleå, Sweden, 2015, p. XT02.pdf..
[22] W.A.J. Albert, Uber Treibseile am Harz. Archiv fur Mineralogie, Georgnosie. *Bergbau und Huttenkunde* 10 (1837) 215–234.
[23] A. Wöhler, Ueber die Festigkeits-Versuche mit Eisen und Stahl, Zeitschrift für das Bauwesen 20 (1870) 73–106.
[24] J.L. Van Ornum, The fatigue of cement products, Transactions of the American Society of Civil Engineers 51 (2) (1903) 443–445.
[25] W.K. Hatt, Fatigue of concrete, In *Highway Research Board Proceedings* 4 (1925) 47–60.
[26] H.F. Clemmer, Fatigue of concrete, Proceedings, ASTM 22 (1922) 408–417.
[27] K. Aas-Jakobsen, R. Lenschow, Behavior of reinforced columns subjected to fatigue loading, In *Journal Proceedings* 70 (1973) 199–206.
[28] R. Tepfers, T. Kutti, Fatigue strength of plain, ordinary, and lightweight concrete, ACI Journal Proceedings 76 (5) (1979) 635–652.
[29] fib B52 (2010): Structural Concrete. Textbook on behavior, design and performance. 2nd Ed., Volume 2: 4. Basis of design. Lausanne: The International Federation for Structural Concrete (fib), January 2010, 340 pp, ISBN 978-2-88394-092-5.
[30] EC2 (2004-2006): Eurocode 2: Design of concrete structures, EN 1992. Part 1: General rules; Part 2(2005): Concrete Bridges; Part 3(2006): Liquid containment structures.
[31] H. Matsushita, Y. Tokumitsu, A STUDY ON COMPRESSIVE FATIGUE STRENGTH OF CONCRETE CONSIDERED SURVIVAL PROBABILITY, Proceedings of the Japan Society of Civil Engineers 1979 (284) (1979) 127–138.
[32] J.K. Kim, Y.Y. Kim, Experimental study of the fatigue behavior of high strength concrete, Cement and Concrete Research 26 (10) (1996) 1513–1523.
[33] T.T. Hsu, Fatigue of plain concrete, ACI Journal Proceedings 78 (4) (1981) 292–305.
[34] F.Z. Kachkouch, C.C. Noberto, L.F. de Albuquerque Lima Babadopulos, A.R. S. Melo, A.M.L. Machado, N. Sebaibi, F. Boukhelf, Y. El Mendili, Fatigue behavior of concrete: A literature review on the main relevant parameters, Construction and Building Materials 338 (2022) 127510.
[35] R. Tepfers, Tensile fatigue strength of plain concrete, ACI Journal Proceedings 76 (8) (1979) 919–934.
[36] H.A.W. Cornelissen, H.W. Reinhardt, Uniaxial tensile fatigue failure of concrete under constant-amplitude and programme loading, Magazine of Concrete Research 36 (129) (1984) 216–226.
[37] H. Thun, U. Ohlsson, L. Elfgren, A deformation criterion for fatigue of concrete in tension, Structural Concrete 12 (3) (2011) 187–197.
[38] G.L. Balazs, Fatigue of bond. *Materials Journal* 88 (6) (1992) 620–630.
[39] H. Thun, Assessment of fatigue resistance and strength in existing concrete structures, Luleå University of Technology, Sweden, 2006. PhD Thesis, Division. of Structural Engineering.
[40] M.A. Miner, Cumulative damage in fatigue, Journal of Applied Mechanics 12 (3) (1945) 159–164.
[41] S. Manson, J. Freche, C. Ensign, Application of a double linear damage rule to cumulative fatigue, Fatigue Crack Propagation 415 (1967) 384–412.
[42] B.H. Oh, Cumulative damage theory of concrete under variable-amplitude fatigue loadings, ACI Materials Journal 88 (1) (1991) 41–48.
[43] Wei, X., Makhloof, D. A., & Ren, X. (2022). Analytical models of concrete fatigue: A state-of-the-art review. *Computer Modeling in Engineering and Sciences*, 2022.
[44] Y. Yao, L. Wang, F.H. Wittmann, N. De Belie, E. Schlangen, C. Gehlen, Z.D. Wang, H.E. Alava, Y. Cao, B.M.D. Yunus, J. Li, Recommendation of RILEM TC 246-TDC: test methods to determine durability of concrete under combined environmental actions and mechanical load, Materials and Structures 50 (2) (2017) 1–9.
[45] U. Schneider, S.W. Chen, The chemomechanical effect and the mechanochemical effect on high-performance concrete subjected to stress corrosion, Cement and Concrete Research 28 (4) (1998) 509–522.
[46] H. Wang, C. Lu, W. Jin, Y. Bai, Effect of external loads on chloride transport in concrete, Journal of Materials in Civil Engineering 23 (7) (2011) 1043–1049.
[47] Y. Ren, Q. Huang, Q.Y. Liu, J.Z. Sun, X.L. Liu, Chloride ion diffusion of structural concrete under the coupled effect of bending fatigue load and chloride, Materials Research Innovations 19 (sup1) (2015) S1–181.
[48] D. Yu, B. Guan, R. He, R. Xiong, Z. Liu, Sulfate attack of Portland cement concrete under dynamic flexural loading: A coupling function, Construction and Building Materials 115 (2016) 478–485.
[49] W. Li, Z. Jiang, Z. Yang, J. Jiang, W. Sun, Z. Deng, Interactive effect of mechanical fatigue load and the fatigue effect of freeze-thaw on combined damage of concrete, Journal of Materials in Civil Engineering 27 (8) (2015) 04014230.
[50] Y. Qiao, W. Sun, J. Jiang, Damage process of concrete subjected to coupling fatigue load and freeze/thaw cycles, Construction and Building Materials 93 (2015) 806–811.
[51] A. Shen, S. Lin, Y. Guo, T. He, Z. Lyu, Relationship between flexural strength and pore structure of pavement concrete under fatigue loads and Freeze-thaw interaction in seasonal frozen regions, Construction and Building Materials 174 (2018) 684–692.
[52] B. Lei, W. Li, Z. Luo, X. Li, V.W. Tam, Z. Tang, Performance deterioration of sustainable recycled aggregate concrete under combined cyclic loading and environmental actions, Journal of Sustainable Cement-Based Materials 10 (1) (2021) 23–45.
[53] P. Zhang, S. Ren, Y. Zhao, L. Wang, N. Long, F. Chen, C. Liu, Combined effects of sulfate attack under drying–wetting cycles and loading on the fatigue behavior of concrete, Advances in Structural Engineering 24 (16) (2021) 3825–3836.
[54] C.-S. Lee, I.-S. Yoon, Prediction of carbonation progress for concrete structures considering change of atmospheric environment, Journal of the Korea Concrete Institute 15 (4) (2003) 574–584.
[55] S. Hussain, D. Bhunia, S.B. Singh, Comparative study of accelerated carbonation of plain cement and fly-ash concrete, Journal of Building Engineering 10 (2017) 26–31.
[56] V.G. Papadakis, C.G. Vayenas, M.N. Fardis, A reaction engineering approach to the problem of concrete carbonation, AIChE Journal 35 (10) (1989) 1639–1650.
[57] E.I. Moreno E. Cob-Sarabia P.C. Borges Corrosion rates from carbonated concrete specimens Corrosion 2004 2004 OnePetro.
[58] K. Suda, S. Misra, K. Motohashi, Corrosion products of reinforcing bars embedded in concrete, Corrosion Science 35 (5–8) (1993) 1543–1549.
[59] P. Liu, Y. Chen, Z. Yu, Effects of temperature, relative humidity and carbon dioxide concentration on concrete carbonation, Magazine of Concrete Research 72 (18) (2020) 936–947.
[60] E. Bastidas-Arteaga, G. Rianna, H. Gervasio, M. Nogal, Multi-region lifetime assessment of reinforced concrete structures subjected to carbonation and climate change, Structures 45 (2022) 886–899.
[61] S. Alahmad, A. Toumi, J. Verdier, R. François, Effect of crack opening on carbon dioxide penetration in cracked mortar samples, Materials and Structures 42 (5) (2009) 559–566.
[62] K. Tanaka, T. Nawa, H. Hashida, J.H. Jeon, Effect of repeated load on micro structure and carbonation of concrete and mortar, In *Eighth International Conference on Durability of Building Materials and Components* (1999) 256–265.
[63] J.Y. Jiang, W. Sun, J.P. Liu, J. Wang, C.C. Chen, Fatigue durability of steel fiber reinforced concrete with super-high vertical pumping distance, *Journal of Southeast University (Natural Science Edition)* 36 (S2) (2006) 259–262. In Chinese.
[64] J. Wang, Effects of fatigue damage and cracks on concrete durability, Southeast University, Nanjing, China, 2008. Master's Thesis,(In Chinese.
[65] C. Jiang, X. Gu, W. Zhang, W. Zou, Modeling of carbonation in tensile zone of plain concrete beams damaged by cyclic loading, Construction and Building Materials 77 (2015) 479–488.
[66] Y.X. Zhou, D.T. Niu, Y.Y. Miao, X.Y. Lu, An experimental study of carbonation of concrete under flexural fatigue, Industrial Construction 46 (8) (2016) 123–126. In Chinese.

[67] C. Jiang, Q. Huang, X. Gu, W. Zhang, Experimental investigation on carbonation in fatigue-damaged concrete, Cement and Concrete Research 99 (2017) 38–52.
[68] J. Han, W. Liu, S. Wang, D.S. Geert, W. Sun, Y. Liang, Carbonation reaction and microstructural changes of metro-tunnel segment concrete coupled with static and fatigue load, Journal of Materials in Civil Engineering 29 (2) (2017) 04016216.
[69] L. Song, J.L. Liu, C.X. Cui, Z.W. Yu, Z.W. Fan, J. Hou, Carbonation process of reinforced concrete beams under the combined effects of fatigue damage and environmental factors, Applied Sciences 10 (11) (2020) 3981.
[70] J.Y. Jiang, Service performance of HPSFRC suitable for super-high vertical pumping, Southeast University, Nanjing, China, 2008. PhD Thesis,(In Chinese.
[71] Y.Y. Miao, D.T. Niu, N. Cheng, Durability of concrete under the combined action of carbonization and fatigue loading of vehicles, Science of Advanced Materials 11 (12) (2019) 1781–1787.
[72] C. Jiang, Q.H. Huang, X.L. Gu, W.P. Zhang, Modeling the effects of fatigue damage on concrete carbonation, Construction and Building Materials 191 (2018) 942–962.
[73] K. Tuutti, Corrosion of steel in concrete, Swedish Cement and Concrete Research Institute, Stockholm, 1982. Report No.CBI Research 4,.
[74] V.G. Papadakis, C.G. Vayenas, M.N. Fardis, Fundamental modeling and experimental investigation of concrete carbonation, Materials Journal 88 (4) (1991) 363–373.
[75] X. Zhang, X. Zhou, H. Zhou, K. Gao, Z. Wang, Studies on forecasting of carbonation depth of slag high performance concrete considering gas permeability, Applied Clay Science 79 (2013) 36–40.
[76] D.T. Niu, Z.P. Dong, J.X. Pu, Random model of predicting the carbonated concrete depth, Industrial Construction 29 (9) (1999) 41–45.
[77] L. Jiang, B. Lin, Y. Cai, A model for predicting carbonation of high-volume fly ash concrete, Cement and Concrete Research 30 (5) (2000) 699–702.
[78] M. Guiglia, M. Taliano, Comparison of carbonation depths measured on in-field exposed existing RC structures with predictions made using fib-Model Code 2010, Cement and Concrete Composites 38 (2013) 92–108.
[79] D. Chen, S. Liu, J. Shen, G. Sun, J. Shi, Experimental study and modelling of concrete carbonation under the coupling effect of freeze-thaw cycles and sustained loads, Journal of Building Engineering 52 (2022) 104390.
[80] J. Wang, H. Su, J. Du, Influence of coupled effects between flexural tensile stress and carbonation time on the carbonation depth of concrete, Construction and Building Materials 190 (2018) 439–451.
[81] Alexeyev. Corrosion of reinforcement in reinforced concrete structures and protection of [M]. Translated by Wu Xingzu et al., Beijing: China Building Industry Press, 1983.
[82] B. Gérard, J. Marchand, Influence of cracking on the diffusion properties of cement-based materials: Part I: Influence of continuous cracks on the steady-state regime, Cement and Concrete Research 30 (1) (2000) 37–43.
[83] H.W. Song, S.J. Kwon, K.J. Byun, C.K. Park, Predicting carbonation in early-aged cracked concrete, Cement and Concrete Research 36 (5) (2006) 979–989.
[84] B. Martın-Pérez, H. Zibara, R.D. Hooton, M.D.A. Thomas, A study of the effect of chloride binding on service life predictions, Cement and Concrete Research 30 (8) (2000) 1215–1223.
[85] C.A. Apostolopoulos, S. Demis, V.G. Papadakis, Chloride-induced corrosion of steel reinforcement–Mechanical performance and pit depth analysis, Construction and Building Materials 38 (2013) 139–146.
[86] A. Neville, Chloride attack of reinforced concrete: an overview, Materials and Structures 28 (2) (1995) 63–70.
[87] H.W. Song, H.B. Shim, A. Petcherdchoo, S.K. Park, Service life prediction of repaired concrete structures under chloride environment using finite difference method, Cement and Concrete Composites 31 (2) (2009) 120–127.
[88] MARIO Collepardi, ALDO Marcialis, RENATO Turriziani, Penetration of chloride ions into cement pastes and concretes, Journal of the American Ceramic Society 55 (10) (1972) 534–535.
[89] P.S. Mangat, B.T. Molloy, Prediction of long term chloride concentration in concrete, Materials and Structures 27 (6) (1994) 338–346.
[90] L.O. Nillson M. Massat L. Tang The effect of non-line chloride binding on the predication of chloride penetration into concrete structures V.M. Malhotra Durability of Concrete, ACI sp-145 1994 Detroit 469 486.
[91] W. Chalee, C.A. Jaturapitakkul, P. Chindaprasirt, Predicting the chloride penetration of fly ash concrete in seawater, Marine Structures 22 (3) (2009) 341–353.
[92] S. Caré, Influence of aggregates on chloride diffusion coefficient into mortar, Cement and Concrete Research 33 (7) (2003) 1021–1028.
[93] A. Boddy, E. Bentz, M.D.A. Thomas, R.D. Hooton, An overview and sensitivity study of a multimechanistic chloride transport model, Cement and Concrete Research 29 (6) (1999) 827–837.
[94] W. Wongkeo, P. Thongsanitgarn, A. Ngamjarurojana, A. Chaipanich, Compressive strength and chloride resistance of self-compacting concrete containing high level fly ash and silica fume, Materials and Design 64 (2014) 261–269.
[95] A.D. Tegguer, S. Bonnet, A. Khelidj, V. Baroghel-Bouny, Effect of uniaxial compressive loading on gas permeability and chloride diffusion coefficient of concrete and their relationship, Cement and Concrete Research 52 (2013) 131–139.
[96] W. Ahn, D.V. Reddy, Galvanostatic testing for the durability of marine concrete under fatigue loading, Cement and Concrete Research 31 (3) (2001) 343–349.
[97] M. Saito, H. Ishimori, Chloride permeability of concrete under static and repeated compressive loading, Cement and Concrete Research 25 (4) (1995) 803–808.
[98] Z. Song, L. Jiang, W. Li, C. Xiong, H. Chu, Impact of compressive fatigue on chloride diffusion coefficient in OPC concrete: An analysis using EIS method, Construction and Building Materials 113 (2016) 712–720.
[99] Y. Li, A. Shen, Z. Lyu, Y. Guo, Investigations of chloride ions permeability of pavement concrete under coupled effect of fatigue loading and hydrodynamic pressure, International Journal of Pavement Engineering 23 (5) (2022) 1659–1674.
[100] D.M. Yu, Research on chloride ion transport behaviour and model of concrete under coupling of fatigue load and environment, Chang'an University, Xi'an, China, 2017. PhD Thesis,(In Chinese.
[101] J. Wu, R. Zhang, B. Diao, W. Zhang, J. Xu, Effects of pre-fatigue damage on high-cycle fatigue behavior and chloride permeability of RC beams, International Journal of Fatigue 122 (2019) 9–18.
[102] J. Wu, J. Xu, B. Diao, D.K. Panesar, Chloride diffusivity, fatigue life, and service life analysis of RC beams under chloride exposure, Journal of Materials in Civil Engineering 32 (6) (2020) 04020107.
[103] Z.J. Liu B.o. Diao X.N. Zheng Degradation Mechanism of Reinforced Concrete Beam Subjected to Fatigue Loads and Seawater Erosion AMM 744-746 38 45.
[104] C. Fu, H. Ye, X. Jin, D. Yan, N. Jin, Z. Peng, Chloride penetration into concrete damaged by uniaxial tensile fatigue loading, Construction and Building Materials 125 (2016) 714–723.
[105] D.T. Niu, X.Y. Lu, Y.Y. Miao, Y.X. Zhou, Diffusion of chloride ions into fatigue-damaged concrete in salt spray environment, *Journal of Xi'an University of Architecture and Technology (Natural Science Edition)* 47 (5) (2015) 617–620.
[106] J. Wu, B.o. Diao, Y. Cao, J. Zhong, X. Shi, Chloride concentration distributions in fatigue damaged RC beams revealed by energy-dispersive X-ray spectroscopy, Construction and Building Materials 234 (2020) 117396.
[107] J. Wu, J. Xu, B.o. Diao, D.K. Panesar, Impacts of reinforcement ratio and fatigue load level on the chloride ingress and service life estimating of fatigue loaded reinforced concrete (RC) beams, Construction and Building Materials 266 (2021) 120999.
[108] J. Wu, B. Diao, W. Zhang, Y. Ye, Z. Liu, D. Wang, Chloride diffusivity and service life prediction of fatigue damaged RC beams under seawater wet-dry environment, Construction and Building Materials 171 (2018) 942–949.
[109] C. Wang, W. Sun, J. Jiang, J. Han, B. Ye, Chloride ion transport performance in slag mortar under fatigue loading, Science China Technological Sciences 55 (5) (2012) 1359–1364.
[110] X.H. Wang, B. Chen, Y. Gao, J. Wang, L. Gao, Influence of external loading and loading type on corrosion behavior of RC beams with epoxy-coated reinforcements, Construction and Building Materials 93 (2015) 746–765.
[111] L. Jiang, C. Li, C. Zhu, Z. Song, H. Chu, The effect of tensile fatigue on chloride ion diffusion in concrete, Construction and Building Materials 151 (2017) 119–126.
[112] N. Jiang, Y. Liu, Y. Deng, F. Yu, Reliability assessment of concrete under chloride penetration and fatigue loading based on copula function, Journal of Materials in Civil Engineering 32 (12) (2020) 04020366.
[113] C. Wang, W. Sun, J. Jiang, Chloride ion transport in fly ash mortar under action of fatigue loading, Journal of Wuhan University of Technology-Mater. Sci. Ed. 27 (6) (2012) 1165–1171.
[114] B. Gerard, G. Pijaudier-Cabot, C. Laborderie, Coupled diffusion-damage modelling and the implications on failure due to strain localization, International Journal of Solids and Structures 35 (31–32) (1998) 4107–4120.
[115] T. Xiang, R. Zhao, Reliability evaluation of chloride diffusion in fatigue damaged concrete, Engineering Structures 29 (7) (2007) 1539–1547.
[116] J.Y. Jiang, W. Sun, J. Wang, C.H. Wang, Resistance to chloride ion diffusion of structural concrete under bending fatigue load, *Journal of Southeast University (Natural Science Edition)* 40 (2) (2010) 362–366. In Chinese.
[117] T. Yang, B. Guan, G. Liu, Y. Jia, Modeling of chloride ion diffusion in concrete under fatigue loading, KSCE Journal of Civil Engineering 23 (1) (2019) 287–294.
[118] Fagerlund, G. (1994). Influence of environmental factors on the frost resistance of concrete: a contribution to the BRITE/EURAM project BREU-CT92-0591" The Residual Service Life of Concrete Structures". Report TVBM, 3059, Lund University, Lund.
[119] Z. Yang, W.J. Weiss, J. Olek, Water transport in concrete damaged by tensile loading and freeze-thaw cycling, Journal of Materials in Civil Engineering 18 (3) (2006) 424–434.
[120] G. Fagerlund Service life with regard to frost attack: a probabilistic approach M.A. Lacasse D.J. Vainer Durability of Building Materials and Components 8, Institute for Research in Construction, Ottawa ON, K1A 0R6 1999 Canada 1268 1279.
[121] T.C. Powers, A working hypothesis for further studies of frost resistance of concrete, In *Journal Proceedings* 41 (1) (1945) 245–272.
[122] T.C. Powers, R.A. Helmuth, Theory of volume changes in hardened Portland-cement paste during freezing, In *Highway Research Board Proceedings* 32 (1953) 286–297.
[123] F. Gong, S. Jacobsen, Modeling of water transport in highly saturated concrete with wet surface during freeze/thaw, Cement and Concrete Research 115 (2019) 294–307.
[124] X.-C. Qin, S.-P. Meng, D.-f. Cao, Y.-M. Tu, N. Sabourova, N. Grip, U. Ohlsson, T. Blanksvärd, G. Sas, L. Elfgren, Evaluation of freeze-thaw damage on concrete material and prestressed concrete specimens, Construction and Building Materials 125 (2016) 892–904.
[125] Z. Liu, W. Hansen, Freezing characteristics of air-entrained concrete in the presence of deicing salt, Cement and Concrete Research 74 (2015) 10–18.
[126] W.L. Qiu, F. Teng, S.S. Pan, Damage constitutive model of concrete under repeated load after seawater freeze-thaw cycles, Construction and Building Materials 236 (2020), 117560.

[127] F. Liu, Z. You, X. Yang, H. Wang, Macro-micro degradation process of fly ash concrete under alternation of freeze-thaw cycles subjected to sulfate and carbonation, Construction and Building Materials 181 (2018) 369–380.
[128] Y.i. Wang, J. Li, T. Ueda, D. Zhang, J. Deng, Meso-scale mechanical deterioration of mortar subjected to freeze thaw cycles and sodium chloride attack, Cement and Concrete Composites 117 (2021) 103906.
[129] Q.H. Xiao, Z.Y. Cao, X. Guan, Q. Li, X.L. Liu, Damage to recycled concrete with different aggregate substitution rates from the coupled action of freeze-thaw cycles and sulfate attack, Construction and Building Materials 221 (2019) 74–83.
[130] M. Nili, A. Azarioon, S.M. Hosseinian, Novel internal-deterioration model of concrete exposed to freeze-thaw cycles, Journal of Materials in Civil Engineering 29 (9) (2017) 04017132.
[131] P. Soroushian, M. Elzafraney, Damage effects on concrete performance and microstructure, Cement and Concrete Composites 26 (7) (2004) 853–859.
[132] D.P. Forgeron, J.F. Trottier, Evaluating the effects of combined freezing and thawing and flexural fatigue loading cycles on the fracture properties of FRC, WIT Transactions on The Built Environment 76 (2004) 117–187.
[133] M. Hasan, T. Ueda, Y. Sato, Stress-strain relationship of frost-damaged concrete subjected to fatigue loading, Journal of Materials in Civil Engineering 20 (1) (2008) 37–45.
[134] W. Li, W. Sun, J. Jiang, Damage of concrete experiencing flexural fatigue load and closed freeze/thaw cycles simultaneously, Construction and Building Materials 25 (5) (2011) 2604–2610.
[135] W. Li, W. Sun, J. Jiang, Damage of concrete subjected to simultaneous fatigue load and thermal effect, Magazine of Concrete Research 64 (1) (2012) 35–42.
[136] R.G. Liu, T. Liu, W.L. Zhou, Y.D. Zhang, Y. Chen, Freeze-thaw cycle test and damage mechanics model of PC members after fatigue loads, *Journal of Nanjing University of Technology (Natural Science Edition)* 33 (3) (2011) 22–27. In Chinese.
[137] J.X. Hong, C.W. Miao, W. Huang, J.P. Liu, Y. Wan, Influence of freeze-thaw damage on the fatigue life of concrete, China Civil Engineering Journal 45 (6) (2012) 83–89. In Chinese.
[138] J.G. Jang, H.K. Kim, T.S. Kim, B.J. Min, H.K. Lee, Improved flexural fatigue resistance of PVA fiber-reinforced concrete subjected to freezing and thawing cycles, Construction and Building Materials 59 (2014) 129–135.
[139] Z. Liu, B.o. Diao, X. Zheng, Effects of seawater corrosion and freeze-thaw cycles on mechanical properties of fatigue damaged reinforced concrete beams, Advances in Materials Science and Engineering 2015 (2015) 1–15.
[140] Y.C. Guo, A.Q. Shen, T.Q. He, S.B. Zhou, Micro-crack propagation behaviour of pavement concrete subjected to coupling effect of fatigue load and freezing-thawing cycles, Journal of Traffic and Transportation Engineering 16 (5) (2016) 1–9. In Chinese.
[141] Y.C. Guo, A.Q. Shen, T.Q. He, S.B. Zhou, B. Wang, Pore structures research on pavement cement concrete subjected to coupling effect of fatigue load and cyclic freeze-thaw in seasonally frozen ground region, China Journal of Highway and Transport 29 (8) (2016) 29–35. In Chinese.
[142] X. Yang, A. Shen, Y. Guo, S. Zhou, T. He, Deterioration mechanism of interface transition zone of concrete pavement under fatigue load and freeze-thaw coupling in cold climatic areas, Construction and Building Materials 160 (2018) 588–597.
[143] Y. Qiao, W. Sun, J. Jiang, D. Pan, Coupling mechanism of saturated concrete subjected to simultaneous fatigue loading and freeze-thaw cycles, Journal of Wuhan University of Technology-Mater. Sci. Ed. 33 (5) (2018) 1121–1128.
[144] J. Lu, K. Zhu, L. Tian, L. Guo, Dynamic compressive strength of concrete damaged by fatigue loading and freeze-thaw cycling, Construction and Building Materials 152 (2017) 847–855.
[145] W. Li, L. Cai, Y. Wu, Q. Liu, H. Yu, C. Zhang, Assessing recycled pavement concrete mechanical properties under joint action of freezing and fatigue via RSM, Construction and Building Materials 164 (2018) 1–11.
[146] A.J. Boyd A. Leone Effect of freeze-thaw cycling on fatigue behavior in concrete 652 2019 IOP Publishing 012028.
[147] M. Haghnejad, A. Modarres, Effect of freeze-thaw cycles on the response of roller compacted concrete pavement reinforced by recycled polypropylene fibre under monotonic and cyclic loadings, Road Materials and Pavement Design 22 (12) (2021) 2704–2720.
[148] J. Yang, T. Zhang, Q. Sun, Experimental study on flexural fatigue properties of reinforced concrete beams after salt freezing, Advances in Materials Science and Engineering 2020 (2020) 1–15.
[149] Y. Zheng, L. Yang, P. Guo, P. Yang, Fatigue characteristics of prestressed concrete beam under freezing and thawing cycles, Advances in Civil Engineering 2020 (2020) 1–11.
[150] B. Chen, J. Wang, A. De Jesus, Flexural fatigue life reliability of alkali-activated slag concrete freeze-thaw damage in cold areas, Advances in Materials Science and Engineering 2021 (2021) 1–20.
[151] Z. Li, Y. Guo, B. Xie, L. Zhou, Z. Chen, Performance attenuation and mechanism of basalt-fibre-reinforced concrete under fatigue load and freeze–thaw cycles, International Journal of Pavement Engineering 1–12 (2022), https://doi.org/10.1080/10298436.2022.2032700.
[152] P.J. Monteiro, A.I. Rashed, J. Bastacky, T.L. Hayes, Ice in cement paste as analysed in the low-temperature scanning electron microscope, Cement and Concrete Research 19 (2) (1989) 306–314.
[153] S. Jacobsen, E.J. Sellevold, S. Matala, Frost durability of high strength concrete: effect of internal cracking on ice formation, Cement and Concrete Research 26 (6) (1996) 919–931.
[154] E. Ballatore, P. Bocca, Variations in the mechanical properties of concrete subjected to low cyclic loads, Cement and Concrete Research 27 (3) (1997) 453–462.
[155] J. Yuan, X. Chen, S. Guo, Experimental study on cyclic tensile behaviour of air-entrained concrete after frost damage, Sādhanā 44 (8) (2019) 1–15.
[156] B. Lei, W. Li, Z. Tang, V.W. Tam, Z. Sun, Durability of recycled aggregate concrete under coupling mechanical loading and freeze-thaw cycle in salt-solution, Construction and Building Materials 163 (2018) 840–849.
[157] M. El-Hawary, A. Al-Sulily, Internal curing of recycled aggregates concrete, Journal of Cleaner Production 275 (2020) 122911.
[158] R.G. Liu, K. Fu, T.C. Yan, Y. Chen, Durability life prediction of prestressed concrete structures in an erosive environment with fatigue subjoining freezing-thawing circle, Journal of Building Structures 30 (3) (2009) 79–86. In Chinese.
[159] W. Dong, X.D. Shen, H.J. Xue, J. He, Y. Liu, Research on the freeze-thaw cyclic test and damage model of Aeolian sand lightweight aggregate concrete, Construction and Building Materials 123 (2016) 792–799.
[160] M. Collepardi, A state-of-the-art review on delayed ettringite attack on concrete, Cement and Concrete Composites 25 (4–5) (2003) 401–407.
[161] P.K. Mehta, Mechanism of sulphate attack on Portland cement concrete—Another look, Cement and Concrete Research 13 (3) (1983) 401–406.
[162] F. Liu, Z. You, A. Diab, Z. Liu, C. Zhang, S. Guo, External sulphate attack on concrete under combined effects of flexural fatigue loading and drying-wetting cycles, Construction and Building Materials 249 (2020), 118224.
[163] A.J. Boyd, S. Mindess, The use of tension testing to investigate the effect of W/C ratio and cement type on the resistance of concrete to sulphate attack, Cement and Concrete Research 34 (3) (2004) 373–377.
[164] M. Santhanam, M.D. Cohen, J. Olek, Sulphate attack research—whither now? Cement and Concrete Research 31 (6) (2001) 845–851.
[165] Rasheeduzzafar, Al-Amoudi, O. S. B., Abduljauwad, S. N., & Maslehuddin, M. (1994). Magnesium-sodium sulphate attack in plain and blended cements. *Journal of Materials in Civil Engineering*, 6(2), 201-222.
[166] A. Neville, The confused world of sulphate attack on concrete, Cement and Concrete Research 34 (8) (2004) 1275–1296.
[167] R. Gao, Q. Li, S. Zhao, Concrete deterioration mechanisms under combined sulphate attack and flexural loading, Journal of Materials in Civil Engineering 25 (1) (2013) 39–44.
[168] U. Schneider, W.G. Piasta, The behaviour of concrete under Na_2SO_4 solution attack and sustained compression or bending, Magazine of concrete research 43 (157) (1991) 281–289.
[169] H. Zhao R. Xiong B.W. Guan Fatigue Damage Property of Cement Concrete under Magnesium Sulfate Corrosion Condition AMM 638-640 1153 1157.
[170] T. Long, H. Zhang, Y. Chen, Z. Li, J. Xu, X. Shi, Q. Wang, Effect of sulphate attack on the flexural fatigue behaviour of fly ash–based geopolymer concrete, The Journal of Strain Analysis for Engineering Design 53 (8) (2018) 711–718.
[171] X. Yan, G. Yang, L. Jiang, Z. Song, M. Guo, Y. Chen, Influence of compressive fatigue on the sulphate resistance of slag contained concrete under steam curing, Structural Concrete 20 (5) (2019) 1572–1582.
[172] M.Z.Y. Ting, K.S. Wong, M.E. Rahman, M.S. Joo, Cyclic compressive behaviour of limestone and silicomanganese slag concrete subjected to sulphate attack and wetting-drying action in marine environment, Journal of Building Engineering 44 (2021), 103357.
[173] L.F. Tietze, C. Ott, K. Gerke, M. Buback, The first example of an increase in the enantioselectivity of a chemical reaction in the presence of a chiral Lewis acid under high pressure, Angewandte Chemie International Edition in English 32 (10) (1993) 1485–1486.
[174] C. Ouyang, A. Nanni, W.F. Chang, Internal and external sources of sulphate ions in Portland cement mortar: two types of chemical attack, Cement and concrete research 18 (5) (1988) 699–709.
[175] C. Plowman, J.G. Cabrera, Mechanism and kinetics of hydration of C_3A and C_4AF. Extracted from cement, Cement and Concrete Research 14 (2) (1984) 238–248.
[176] Z. Zhang, X. Jin, W. Luo, Long-term behaviours of concrete under low-concentration sulphate attack subjected to natural variation of environmental climate conditions, Cement and Concrete Research 116 (2019) 217–230.
[177] B.W. Guan, S.F. Chen, H.P. Li, R. Xiong, D.M. Yu, Sulphate corrosion life of cement concrete under fatigue load, Journal of Building Materials 15 (3) (2012) 395–398. In Chinese.
[178] Y. Zhou, S. Zheng, L. Chen, L.i. Long, B. Wang, Experimental investigation into the seismic behavior of squat reinforced concrete walls subjected to acid rain erosion, Journal of Building Engineering 44 (2021) 102899.
[179] J. Han, W. Liu, S. Wang, D. Du, F. Xu, W. Li, G. De Schutter, Effects of crack and ITZ and aggregate on carbonation penetration based on 3D micro X-ray CT microstructure evolution, Construction and Building Materials 128 (2016) 256–271.
[180] J. Xu, F. Li, A meso-scale model for analysing the chloride diffusion of concrete subjected to external stress, Construction and Building Materials 130 (2017) 11–21.
[181] X. Shi, Y. Yao, L. Wang, C. Zhang, I. Ahmad, A modified numerical model for predicting carbonation depth of concrete with stress damage, Construction and Building Materials 304 (2021) 124389.
[182] X.C. Qin, Research of freeze-thaw mechanism and durability evaluation of concrete and prestressed concrete, Southeast University, Nanjing, China, 2016. PhD Thesis,(In Chinese.
[183] V. Afroughsabet, L. Biolzi, T. Ozbakkaloglu, High-performance fiber-reinforced concrete: a review, Journal of Materials Science 51 (14) (2016) 6517–6551.
[184] M.C. Juenger, R. Siddique, Recent advances in understanding the role of supplementary cementitious materials in concrete, Cement and Concrete Research 78 (2015) 71–80.